Drd1 in the SCN and ARC: Findings from Patch Clamp Electrophysiology Studies of the Hypothalamus

Sean Chadwick
B.S. College of William and Mary, 2015

A Dissertation presented to the Graduate Faculty
of the University of Virginia in Candidacy
for the Degree of Doctor of Philosophy

Department of Biology

University of Virginia
November 2021

Committee Members:
Ali Güler (Advisor)
Ignacio Provencio (First reader)
Masashi Kawasaki
Manoj Patel
Chris Deppmann

Abstract

The hypothalamus integrates sensory and peripheral signals to maintain essential homeostatic functions throughout the body. With respect to sleep and wakefulness, the suprachiasmatic nucleus (SCN) acts as the body's primary central clock and manages the timing of essential behavior and physiological processes. With respect to appetite and food intake, the arcuate nucleus (ARC) acts as the primary mediator of homeostatic feeding, driving food intake behaviors when energy balance is low. Hypothalamic circuits controlling sleep and food intake in mammals are some of the most ancient structures in the mammalian nervous system, however the processes that maintain equilibrium in the wild have not been selected for in the context of modern life. In particular, we lack an understanding of how hedonic processes, such as those regulated by dopamine (DA) and reward systems, impinge on the healthy functioning of hypothalamic circuits in disease. Globally, human diets are increasingly composed of foods rich in fats and sugars, and consumption of these foods results in DA signaling in the midbrain and other regions. Identifying how DA acts on hypothalamic circuits is essential to combating the negative impacts that obesity and circadian dysregulation have on humanity. Here, I investigate the circuitry and signaling in these nuclei relevant to DA and the dopamine 1 receptor (Drd1). My work demonstrates that Drd1 neurons have multimodal and complex actions in hypothalamic nuclei, and modulate important neuronal populations vital to homeostatic processes.

Acknowledgements and Dedication

This work is dedicated to my family. Achieving my PhD would have been impossible without the enormous unconditional support I have received throughout my life from my parents, siblings, and spouse. I also give enormous thanks to my advisor Ali Güler, not just for his enormous patience and dedicated mentorship, but for never ceasing to push me to be a better, more rigorous, and thoughtful scientist. Additionally, I am extremely grateful for the unwavering support and generous attention I have received from my committee members Ignacio Provencio, Masashi Kawasaki, Manoj Patel, and Chris Deppmann throughout my time at UVA. I also extend my sincere gratitude to my colleagues and collaborators, at UVA and elsewhere. In particular, I thank the current and former members of my lab, including Qijun Tang, Ryan Grippo, Everett Altherr, Qi Zhang, Aundrea Rainwater, and Tarun Vippa, whose advice and technical assistance have been instrumental in my work. Finally, I am grateful for my friends (including the furry ones), whose emotional support aided me throughout my graduate career.

Table of Contents

List of Abbreviations

AAV	Adeno associated virus
AC	Adenylyl cyclase
AgRP	Agouti related peptide
ARC	Arcuate nucleus of the hypothalamus
ATP	Adenylyl-tri-phosphate
AVP	Arginine vasopressin
BMAL	Brain and Muscle ARNT-Like 1
cAMP	Cyclic adenosine monophosphate (cAMP)
ChR2	Channelrhodopsin
CLOCK	Circadian locomotor output cycles kaput
CREB	cAMP response element binding
DA	Dopamine
DAG	Diacylglycerol
Drd1	Dopamine 1 receptor
Drd2	Dopamine 2 receptor
DMH	Dorsomedial hypothalamus
GABA	γ-aminobutyric acid
GDP	Guanosine diphosphate
GHSR	Growth Hormone Secretagogue Receptor
GPCR	G-protein coupled receptor
GRP	Gastrin-releasing peptide

GTP	Guanosine triphosphate
HPA	Hypothalamic pituitary axis
IP3	Inositol 1,4,5-trisphosphate
JAK	Janus kinase
MCH4	Melanocortin-4 receptor
NPY	Neuropeptide Y
OVLT	Organum vasculosum lamina terminalis
Per2	Period 2
PIP2	Phosphatidylinositol 4,5-bisphosphate
PKA	Protein kinase A
PK2	Prokineticin 2
PLC	Phospholipase C
PNOC	Prepronociceptin
RHT	Retinohypothalamic tract
RTK	Receptor tyrosine kinase
SCN	Suprachiasmatic nucleus
SPZ	Subparaventricular zone (SPZ)
SST	Somatostatin
STAT	Signal transducer and activator of transcription proteins
TH	Tyrosine hydroxylase
TTFL	Transcriptional/post-translational feedback loop
VIP	Vasoactive intestinal peptide
VPAC2/Vipr2	VIP receptor 2

Chapter 1
Background

Introduction

Health consequences of eating and sleeping disorders

Hunger and sleep are physiological states that drive essential homeostatic behaviors required for survival. In the last 40 years, scientists have identified many neural and molecular processes that underlie circadian and food seeking behaviors, and these mechanisms are highly conserved among rodents, monkeys, humans, and other mammalian species. Today, the worldwide prevalence of sleep and eating disorders in humans is at an all-time high, driven by environmental factors associated with modern life. Sleep disorders such as insomnia, which impacts an estimated 10% to 30% of adults around the world (Bhaskar et al., 2016), have been linked to circadian disruptions caused by artificial light and transmeridian travel. Obesity, now a pandemic, has been driven by a global rise in modern calorie rich diets high in fats and sugars (Kearney, 2010; Statovci et al., 2017). Sleep disorders and obesity can have serious health consequences, and both conditions are associated with increased mortality and decreased quality of life (Li et al., 2014; Parthasarathy et al., 2015). For instance, the consequences of sleep dysregulation include cardiovascular and pulmonary problems, musculoskeletal issues, and decreased immune function (Colten et al., 2006). Comorbid conditions of obesity include increased risk of heart and fatty liver disease, diabetes, and cancer (Bhaskaran

et al., 2014; A. Engin, 2017; Powell-Wiley et al., 2021; Scully et al., 2020). The origins of these disorders are varied, complex, and not fully understood. However, insomnia, jet lag, anorexia, and obesity share the same unifying feature of being diseases whose causes are rooted in the biological activity of the brain. Circadian and feeding behaviors are closely related, and the major neural architectures managing these processes reside within the hypothalamus. Thus, curing humanity of eating and sleeping disorders will require elucidation of the neural mechanisms that are disrupted in affected individuals. This section reviews the current state of knowledge regarding the molecular and neural processes governing circadian rhythms and food intake circuitry, and highlights dopamine's (DA) influence over these processes. We identify several key gaps in our understanding of how hedonic systems influence hypothalamic processes and discuss challenges facing scientists in answering these questions.

Neurons in the hypothalamus control essential homeostatic systems in mammals

The hypothalamus is one of the oldest evolutionary structures in the mammalian nervous system. Located in the basal forebrain, the hypothalamus is a symmetrical region divided by the third ventricle. Hypothalamic neurons mediate numerous homeostatic processes, including thermoregulation and metabolism (Z.-D. Zhao et al., 2017), thirst and electrolyte balance (Leib et al., 2016), mating and reproduction (Robison & Sawyer, 1987; S. X. Zhang et al., 2021), lactation and suckling (Ni et al., 2021), stress responses (M. A. C. Stephens & Wand, 2012), circadian and sleep cycles (Herzog et al., 2017), and hunger and energy equilibrium (Cone et al., 2001). The hypothalamus helps regulate endocrine

systems, in part by direct outputs to the pituitary gland through the hypothalamic pituitary axis (HPA) (Sheng et al., 2020). Autonomic functions are mostly mediated by parasympathetic and sympathetic preganglionic neurons which receive innervations from hypothalamic neurons, controlling essential behaviors during states of rest and arousal, respectively (Iversen et al., 2000).

The hypothalamus integrates peripheral signals and sensory information, allowing hypothalamic nuclei to perform their homeostatic functions in the context of physiological states and environmental cues. The most rostral part of the hypothalamus is directly rostral to the optic chiasm and inferior to the optic tract, and retinal inputs in the retinohypothalamic pathway directly innervate hypothalamic neurons in the suprachiasmatic nucleus (SCN) (Hattar et al., 2006; McNeill et al., 2011). Photic input from the sunlight is the primary *zeitgeber* (German: time giver) which sets the phase of SCN activity, synchronizing animal behavior with time of day. In terms of food intake and metabolism, the arcuate nucleus (ARC), located at the base of the third ventricle and dorsal to the medial eminence, receives numerous peripheral signals relevant to metabolic state and energy balance. Outputs from neurons in the ARC drive or inhibit feeding behaviors.

Negative consequences of obesity

Obesity afflicts millions of people all over the world, and the United States has one of the highest rates of obesity globally. The 2017-2018 National Health and Nutrition Examination Survey found that adjusting for age 42.7% of the adult US population had a BMI of over 30 kg/m2, currently considered by the CDC and WHO to be the threshold for

obesity status (Fryar et al., 2020; Ogden et al., 2020). The obesity pandemic presents an unprecedented challenge for the US healthcare system because being overweight is associated with a variety of severe health risks including cardiovascular disease, diabetes, stroke, and cancer (Bhaskaran et al., 2014). Understanding the root causes of this epidemic is vital to not only improve the health and longevity of Americans but also to ameliorate the massive economic burden obesity places on the public. By one estimate, obesity related US national healthcare costs were calculated at $190.2 billion in 2005 dollars, a staggering 20.6% of the US national healthcare expenditure (Cawley & Meyerfoefer, 2021).

Attributed causes and mechanisms of becoming obese

Evolution has selected for mammalian brain circuits that activate in response to signals of food availability in a given biome. Such neural architecture was likely adaptive in animal populations experiencing food scarcity (Illius et al. 2002), however these systems were not selected for in the context of human food environments enabled by the rise of industry and modern agriculture. This is reflected by the biggest risk factor that leads to obesity: maintenance of rewarding high calorie diets rich in fats and sugars. When coupled with a sedentary lifestyle, individuals with a positive nutrient balance (i.e. higher calorie intake vs energy expenditure) are at the greatest risk of aberrant weight gain (J. O. Hill et al., 2013). Although many factors can contribute to the development of obesity, such as community environments, genetic predispositions, diet exposures in childhood, or drugs and illnesses (van der Valk et al., 2019; Wright & Aronne, 2012), it is ultimately the behavior of the individual that results in obesity. Scientific experiments in rodents and mammals reinforced this: animals which eat more fats and sugars and exercise less,

invariably become overweight and eventually suffer from the same obesity associated health issues as humans (C.-Y. Wang & Liao, 2012). As animals consume highly caloric and rewarding foods, the peripheral and central mechanisms which control appetite and satiation become dysregulated, and feedback systems underpinning energy balance and metabolism become desensitized to high calorie inputs. This phenomenon has been recently linked to changes in dopamine (DA) inputs to the SCN and ARC (Grippo et al., 2017, 2020), as well as changes in outputs from a dopaminergic nucleus in the midbrain, the ventral tegmental area (VTA) (Altherr et al. 2021; Valdivia et al. 2014).

The following sections focus on (1) the organization, structure and function of the ARC, (2) those of SCN, (3) metabotropic signaling including DA and VIP in these areas, and (4) electrophysiological studies and membrane excitability of neurons in these regions.

Arcuate nucleus, food intake, and hedonic feeding

The arcuate nucleus regulates food intake in mammals

In rodents and other mammals, the majority of the attention on central mechanisms underpinning obesogenic behavior has been focused on the arcuate nucleus of the hypothalamus (ARC), a relatively small brain region located at the base of the hypothalamus, directly dorsal to the medial eminence and lateral to the third ventricle. The earliest evidence that the hypothalamus was an important player in food intake behaviors was found by experimenters almost 70 years ago. These experiments found that lesioning various areas in the hypothalamus caused starvation or overeating (Anand

& Brobeck, 1951; Morrison & Mayer, 1957; Teitelbaum & Stellar, 1954), and that stimulation of hypothalamic brain areas could provoke feeding (N. E. Miller, 1960; O. A. Smith, 1956). At this time, researchers speculated that the lateral hypothalamic area (LHA) was the brain region most implicated in this phenomenon (Baillie & Morrison, 1963). However, these experiments likely suffered from challenges due to the relatively primitive technology available at the time used for targeted lesioning of various brain regions in the hypothalamus. The state-of-the-art protocols of the time were imprecise compared to current techniques. Eventually, aided by the development of strategies for generating knockout mice and gene cloning, a proliferation of discoveries regarding the molecular players essential to hypothalamic control of feeding and metabolism occurred in the 1990s. In 1994, researchers cloned the gene for the leptin receptor LepRb (named Ob at that time), identified its hormone ligand leptin, and documented the striking obesity phenotype of leptin receptor knockout animals (Y. Zhang et al., 1994). Simultaneously, researchers identified the orexigenic proteins including the agouti related peptide (AgRP), its cognate receptor melanocortin-4 receptor (MCH4) (Bultman et al., 1992; W. Fan et al., 1997; Huszar et al., 1997; Lu et al., 1994; M. W. Miller et al., 1993), and neuropeptide Y (NPY), which bind a family of receptors known as Y receptors (T. W. Stephens et al., 1995; Yi et al., 2018). Experiments showed that a group of ARC cells marked by expression of AgRP were an essential component of appetite regulation; genetic ablation of these cells resulted in hypophagia and starvation (Gropp et al., 2005; Luquet et al., 2005), while artificial activation of the neurons through optogenetic or chemogenetic techniques induced voracious eating (Aponte et al., 2011; Atasoy et al., 2012; Betley et al., 2013; Krashes et al., 2011). Since then, other neuronal populations participating in

food intake circuitry have been identified, including prepronociceptin-expressing (PNOC) (Jais et al., 2020) and somatostatin-expressing (SST) neurons (S. X. Luo et al., 2018). However, to date no neuronal population has been shown to produce such a profound effect on the feeding behaviors of mammals as that of ARC AgRP/NPY neurons.

Activation AgRP neurons elicits feeding behaviors

Activation of GABAergic ARC AgRP neurons is sufficient to rapidly and reversibly induce feeding in freely awake and moving animals, while activation of POMC neurons inhibits food intake. Studies found the extent of AgRP neuron evoked feeding behaviors are dependent on the activation frequency, irradiance, and expression levels of the optogenic actuator channelrhodopsin 2 (ChR2) in AgRP neurons (Aponte et. al. 2011, Atasoy et. al. 2012). In one in-vivo experiment, a unilateral optical fiber delivering 10 ms square pulses of blue light at 2.0 mW mm^2 onto ChR2 expressing AgRP neurons was shown to significantly increase feeding at frequencies as low as 2 Hz delivered every 10s (Aponte et. al. 2011). This effect on food intake produced increasingly robust effects for 10 Hz and 20 Hz simulations, respectively (Aponte et. al. 2011). While this study found that food intake increased linearly with increasing virally-mediated expression of axonal ChR2 (defined by authors as ChR2 penetrance), it is noteworthy that even relatively high ChR2 penetrance of some brain regions was insufficient to invoke feeding to the same extent as low ChR2 penetrance in other regions, likely reflecting the relative functional importance of different circuit outputs on animal behavior (Aponte et. al. 2011). Parallel findings from patch clamp electrophysiology of AgRP neurons selectively expressing ChR2 in acute brain slices showed that increasing the frequency of stimulation of afferents caused graded increases in GABAergic inhibition of innervated cells in

downstream regions, such as the paraventricular nucleus of the hypothalamus (PVH) (Atasoy et. al. 2012). Remarkably, in this same experiment Atasoy et. al. found that a single 1ms light pulse was capable of producing a multitude of IPSCs that could last up to 1s. Additionally, the strength of the GABAergic input (i.e., the amount of GABA being released by AgRP neurons and subsequent PVH inhibition) increased with successive stimulations and reached a higher steady state for 10 Hz vs 5 Hz stimulation paradigms (Atasoy et. al. 2012).

Outputs of AgRP neurons to downstream regions drives feeding behaviors

AgRP neurons secrete vesicles containing γ-aminobutyric acid (GABA), AgRP, and NPY (Tong et al., 2008). The general connectivity of AgRP neurons has been described with projection tracing and imaging experiments, which identified the paraventricular nucleus (PVH), bed nucleus of the stria terminalis (BNST), lateral hypothalamic area (LHA), periaqueductal gray (PAG), paraventricular thalamus (PVT), and the central nucleus of the amygdala (CEA) as regions innervated by AgRP neurons axons. However, it was not until 2013 that Betley et. al. performed additional experiments to determine which downstream projections are capable of stimulating feeding and which have little or no effect on food intake behavior. AgPR afferents were stimulated via differential placements of the fiber optic over the AgRP::Cre ChR2 terminals and several downstream projection sites were identified where activation of those input fibers is capable of eliciting feeding. These areas include the PVH, BNST, LHA and to some minor extent the PVT. However, the question still remained if the AgRP axonal projections were organized in a ‘one to all’ or ‘one to many’ configurations. In an ‘one to one’ configuration, an individual cell outputs to one distinct area alone (i.e. only to the BNST). In an ‘one to all’ configuration, a given

neurons has afferents and collaterals that project to all downstream target brain regions. (i.e. an AgRP neuron could have projections to both BNST, PVH, LHA, etc.) Experiments using retrograde tracing techniques strongly support the hypothesis that arcuate AgRP cells have a ‘one to one’ connectivity, and lack axon collaterals to other projection areas (Betley et al., 2013). The lack of axon collaterals is particularly important because it would make it less likely that ChR2 stimulation was back propagating action potentials that were resulting in synaptic vesicle release in the whole neuron and its additional projection sites. The approximate stoichiometry of the outputs from AgRP neurons was characterized and so was the stoichiometry of the actual AgRP synapses and collaterals. Roughly 29% of AgRP neurons output to the PVH, 18% output to the BNST, and 2% to 4% of output to the PAG or PVT. Based on their labeling of AgRP neurons, these investigators report their analysis can account for roughly 60% of the outputs of AgRP neurons, of which the remaining 40% of the axon projection destinations are unknown. Negligible or no collateralization was found between target projection sites. Additionally, AgRP neurons were capable of forming multiple synapses on the dendrites and soma of target cells, indicating that the organization of AgRP afferents is parallel and redundant (Betley et al., 2013).

Hedonic vs homeostatic feeding

Studies linking food intake behavior with ARC circuitry has led to the view that AgRP neurons integrate stimuli relevant to the induction or inhibition of homeostatic feeding. This has resulted in categorical classification of inputs as being homeostatic or hedonic in nature. However, distinguishing between inputs regulating energy balance (such as

enteric distension and detection of nutrients in the gut and blood stream), and stimuli associated with pleasure and reward learning mechanisms (generally including sensations of olfaction, palatability, and drug reinforcement) has proved challenging (Berridge et al., 2010; Wise, 2006). Identifying the neural pathways and signals associated with each category of feeding behavior (i.e. homeostatic vs hedonic) remains one of the biggest challenges in elucidating the neural underpinnings of obesogenic behaviors, and the role of dopamine in these processes is reviewed in later sections.

SCN and circadian rhythms

The SCN is the master central clock in the brain

Located in the basal forebrain just above the optic chiasm, the SCN is composed of approximately 20,000 neurons in two symmetrical, tear drop shaped nuclei at the base of the third ventricle. The SCN acts as the main central clock in mammals, where the activity of SCN neurons controls circadian processes in the brain and throughout the body. SCN neurons have been divided into two morphological groups, residing in the shell and core compartments of the SCN. The neural activity of the SCN synchronizes clocks in peripheral tissues, regulating important homeostatic processes including metabolism. SCN neurons are required for most circadian behaviors, including animal locomotion, sleep, and learning (Evans & Davidson, 2013). Ablation of SCN neurons results in loss of rhythmic behaviors and processes (Abe et al., 1979). Most cells in mammalian organisms possess some degree of intrinsic circadian rhythmicity, although clocks in peripheral tissues typically are delayed in their phase by several hours relative to SCN neurons (Buhr & Takahashi, 2013; Welsh et al., 2004). Rhythmic cells are described as cell autonomous oscillators, as dissociated cells maintain individual rhythms in intrinsic membrane excitability and transcription factor turn over (Herzog et al., 2017; Welsh et al., 2004).

Inputs to the SCN set the phase of circadian behaviors

The SCN is sensitive to environmental cues and integrates external signals to synchronize the phase of SCN neurons, and by extension, peripheral tissues to the

prevailing day:night cycle. Environmental stimuli which can provide time-of-day cues and thereby affect the phase of the central clock are called *Zeitgebers* (German: time giver). These include light (R. Y. Moore, 1995), signals of energy state and balance (R. M. Buijs et al., 2006), exercise and locomotion (Power et al., 2010), eating (Koch et al., 2020; Zarrinpar et al., 2016), drinking (C. Gizowski et al., 2016), medications and drugs (Mohawk et al., 2009; Weaver, 1998), and social interactions (Mrosovsky et al., 1989). Light is the most important *Zeitgeber*, synchronizing the phase of the SCN to the astronomical day. Photic information is conveyed from melanopsin expressing neurons in the retina to the SCN by retinohypothalamic tract (RHT) (Hattar et al., 2006). These inputs activate VIP neurons in the SCN, synchronizing individual cell autonomous oscillations (VIP signaling and its consequences for firing rate and synchronization of SCN neurons is discussed in more detail below).

TTFLs control SCN phase and activity

The circadian rhythmicity of mammalian cells, including SCN neurons, is mediated by daily changes in intracellular concentrations of transcription factors, commonly known as clock genes. Two primary transcription factors, CLOCK and BMAL1, promote transcription of other genes which consequently feedback to inhibit their activity. These transcription factors oscillations have a period of approximately 24 hours and are commonly referred to as transcriptional/translational feedback loops (TTFLs) (Buhr & Takahashi, 2013). Circadian TTFLs occur in the majority of cells in the mammalian body, most notably in SCN neurons and cells that comprise peripheral clocks in organs such as the kidney and liver (Herzog et al., 2017). When active, CLOCK and BMAL1 proteins form a heterodimer that drives transcription of *Period* (*Per)* and *Cryptochrome* (*Cry)* genes,

via targeting of E-Box regulatory enhancer domains (Nakahata et al., 2008). Translation of these genes is mediated in part by epigenetic mechanisms including histone deacetylation and acetylation (Nakahata et al., 2008). After being translated, PER and CRY proteins form heterodimers that consequently inhibit CLOCK:BMAL1, resulting in a trough in CLOCK:BMAL1's transcriptional activity. Finally, phosphorylation of PER and CRY targets them for degradation by the 25S proteasome, and CLOCK:BMAL1 function is restored, completing the cycle (Buhr & Takahashi, 2013).

SCN outputs drive circadian processes and behavior

SCN outputs drive circadian processes by providing information about time of day and circadian phase to several important downstream brain regions, including the hippocampus, amygdala, arcuate nucleus, paraventricular nucleus (PVH), dorsomedial hypothalamus (DMH), supraventricular zone (SPZ), and paraventricular nucleus of the thalamus (Harding et al., 2020; Kalsbeek et al., 2006). SCN neurons signal to these targets via a combination of direct synaptic inputs and secreted hormones. Neurotransmitters and peptides released by SCN terminals include vasopressin, GABA, glutamate, arginine vasopressin (AVP) and prokineticin 2 (PK2), and gastrin-releasing peptide (GRP) (Kalsbeek et al., 2006). A well characterized multisynaptic projection to the pineal gland results in the regulation of melatonin production , influencing sleep behaviors. The SCN expresses melatonin receptors, providing feedback signals (Doghramji, 2007) from the pineal. Thirst control is mediated mostly by SCN AVP neurons that innervate the organum vasculosum lamina terminalis (OVLT) (C. Gizowski et al., 2016; Claire Gizowski et al., 2018). The timing of sexual behavior is also regulated in part by SCN outputs (Södersten et al., 1981). Clock phases in peripheral tissues are set by a

mixture of secreted hormones and autonomic outputs (Kalsbeek et al., 2006). The SCN also sends projections to the ARC, helping set daily rhythms in feeding activity (F. N. Buijs et al., 2017).

Metabotropic signaling in the SCN and ARC

Receptor signaling in the hypothalamus

The hypothalamus integrates local and peripheral signals to perform essential homeostatic functions, and hypothalamic nuclei are modulated by a broad array of signaling pathways, including endocrine and metabotropic neurotransmission. G-protein coupled receptors (GPCR), cytokine receptors, and receptor tyrosine kinases (RTK) often mediate metabotropic signaling in different hypothalamic neuronal populations (Nakajima et al., 2016; Park & Ahima, 2014; M. Zhao et al., 2020). GPCR's are integral membrane proteins possessing seven transmembrane domains. Transmembrane domains typically provide specificity to a given GPCR in terms of ligand binding and receptor activation. Intracellular domains of a GPCR interact with a heterotrimeric G protein complex consisting of alpha, beta, and gamma protein subunits. Ligand binding to the GPCR triggers a conformational change in the receptor protein, catalyzing the exchange of guanosine diphosphate (GDP) for guanosine triphosphate (GTP) on the alpha subunit of the G protein. The dissociation of the gamma and beta subunits frees the alpha subunit to mediate intracellular signaling cascades by regulation of enzymes controlling the concentration of second messengers. GPCR pathways are divided generally into three main types on the basis of the second messenger signal that is transduced: activating adenylyl cyclase (Ga/s), inhibiting adenylyl cyclase (Ga/i) or activating phospholipase C (PLC) (Gq/11). Ga/s and Ga/i type GPCRs have opposing functions, where the Ga subunit in these GPCRs either catalyzes or inhibits adenylyl cyclase (AC), which converts adenylyl-triphosphate (ATP) to cyclic adenylyl monophosphate (cAMP). A prominent

consequence of Ga/s signaling is increased kinase activity by protein kinase A (PKA). The regulatory subunit of PKA is bound by cAMP, freeing the catalytic subunit of PKA to perform its kinase functions. cAMP also binds other targets, including transcription factors such as cAMP response element binding (CREB) proteins, which can then target gene regulatory elements and drive transcription. Contrasting this, the alpha subunit of the Gq receptor pathway activates PLC which converts the membrane phospholipid phosphatidylinositol 4,5-bisphosphate (PIP2) into diacylglycerol (DAG) and inositol 1,4,5-trisphosphate (IP3). DAG remains in the membrane where it can bind other proteins, whereas IP3 diffuses into the cytosol. IP3 binds proteins and receptors including IP3-dependent ionotropic calcium channels on intracellular compartments such as the endoplasmic reticulum. Gamma isoforms of PLC can also be activated by TRKs and other kinases (M. Zhao et al., 2020). In canonical cytokine signaling, heteromeric complexes of cytokine receptor subunits provide specificity for the ligand, and generally signal through janus kinase (JAK) and signal transducer and activator of transcription proteins (STATs) (i.e. JAK/STAT) pathways. These families of receptors are large and diverse, and cross talk between signaling pathways is not uncommon. Below we review metabotropic signaling in the SCN and ARC, with a focus on dopamine and VIP signaling.

Structure, function, and relevance of dopamine receptors in hypothalamic processes

Dopamine (DA) is a monoamine neurotransmitter essential in processes of learning, reward, reinforcement, and attention (Missale et al., 1998). Because of its role in addiction and reward, DA has been described as the chief neurotransmitter regulating hedonic

processes, responsible for conveying psychological states of “liking” or “wanting” (Berridge et al., 2010; Berridge & Aldridge, 2008). However, DA’s role in the brain is more complex and varied than simply controlling reward systems, and DA is essential to regulation of many diverse neural processes from locomotion to axonal remodeling (Missale et al., 1998). Drd1 classically has been documented in medium spiny neurons of the striatum which are thought to be reliably identified by their morphology and the presence of inward rectifying Ih currents, which are generated by hyperpolarization-activated cyclic nucleotide-gated (HCN) cation channels. DA receptors are GPCRs which are classified into five families, divided into two groups on the basis of their second messenger signals. Drd1-like receptors include DA receptor 1 and 5 (Drd1, D5R) and signal through Ga/s signaling pathways. D2-like receptors include DA receptors 2, 3, and 4 (D2R, D3R, D4R) and generally signal through opposing Gi pathways (Beaulieu & Gainetdinov, 2011). Some studies have suggested that DA receptors sometimes form multi-receptor complexes, such as Drd1-D2 receptor heteromers, which can signal through Gq signaling, although this is thought to be less common than typical Drd1 and D2-like receptor signaling, and reports on the existence of functional Drd1-D2 receptor complexes are conflicting (Frederick et al., 2015; O’Dowd et al., 2012).

DA has several roles in hypothalamic processes, including mating (S. X. Zhang et al., 2021), lactation (Fitzgerald & Dinan, 2008), circadian rhythms (Grippo et al., 2017), and food intake (Alhadeff et al., 2019; Grippo et al., 2020). The mechanisms through which DA affects hypothalamic cells are diverse and incompletely understood. During mating, hypothalamic DA neurons drive mounting and sniffing behavior through cAMP signaling

in neurons in the medial preoptic area (MPOA) (S. X. Zhang et al., 2021). During lactation, DA acts on D2 receptors, providing a negative feedback loop that opposes actions of the lactation hormone prolactin (Fitzgerald & Dinan, 2008). In the SCN, local increases in DA tone from high fat diet exposure drive phase shifting of the central clock, accelerating entrainment (Grippo et al., 2017). In the ARC feeding circuits, AgRP and POMC neurons respond differentially to DA (X. Zhang & van den Pol, 2016), and responses of orexigenic neurons to gastric fat are dampened by DA antagonists (Alhadeff et al., 2019). Unsurprisingly, psychostimulants and other drugs which act on the dopamine transporter (DAT) and DA neurons can have profound effects on these circuits. Particularly in feeding circuits, the discrete mechanisms mediating DA's role are incompletely characterized. For instance, it is unknown which DAergic neurons release DA to the ARC during food intake, despite evidence suggesting DA's action is only relevant during reward presentation (Alhadeff et al., 2019).

VIP and other metabotropic signaling controls synchronization of SCN clocks

VIP is one of the most important factors regulating SCN neuron phase and synchronization (Hastings et al. 2018). VIP signals to SCN neurons via its cognate receptor VIP receptor 2 (VPAC2) encoded by the *VIPR2* gene (Takeuchi et al., 2020). Additionally, pituitary adenylate cyclase-activating polypeptide (PACAP) released by retinal inputs to the SCN can also signal to SCN neurons by binding VPAC2. The cognate receptor for PACAP is the pituitary adenylate cyclase-activating polypeptide type I receptor isoform 1 (PAC1-R), encoded for by the *PAC1* gene (Hirabayashi et al., 2018). Both PAC1 and VPAC2 are seven transmembrane receptor Ga/s type GPCRs, however, only VPAC2 holds specificity for both PACAP and VIP. Studies of single and double

knockout animals for these receptors revealed that PAC1 is important for integrating photic inputs, while VPAC2 signaling is mostly responsible for phase synchronization of neurons in the SCN (Hannibal et al., 2017). VIP signaling sets the phase of TTFL oscillations by synchronizing Ca+ and cAMP levels between SCN neurons (O'Neill et al., 2013). These second messengers drive expression of Per protein through interactions with cAMP/Ca2+ response elements (CREs), resetting the TTFL and entraining SCN neurons (Tischkau et al., 2003).

AgRP neurons are inhibited by leptin

AgRP neurons are sensitive to a wide range of hormones and neurotransmitters, facilitated by the arcuate's unique anatomical location near the medial eminence and 3rd ventricle, and privileged access to the blood due to the arcuate's unique lack of blood brain barrier. Most notably, AgRP neurons are modulated by leptin and ghrelin, which inhibit and activate AgRP neurons, respectively (Cone et al., 2001). Encoded by the *LEP* gene in humans and *Lep* gene in mice. Leptin is a cytokine hormone secreted by adipose cells and enterocytes, in approximate proportion to the amount of stored triglycerides in adipose tissue. It is highly conserved in mammals (Cammisotto et al., 2005). In mice and humans the leptin protein consists of 167 amino acids and ranges in mass from roughly 16 to 18 kDa depending on species. Structurally, leptin is composed of 5 alpha helices, 4 longer helices and 1 shorter helix, and contains a disulfide bond between residues 117 and 167 (Münzberg & Morrison, 2015). Increased fat stores result in more leptin secretion and over production of leptin in overweight or obese animals is associated with development of leptin insensitivity in obesity and eating disorders (Ewbank et al., 2020). Leptin has a broad range of endocrine effects related to maintenance of energy balance,

glucose metabolism, and feeding behavior. Secreted leptin circulates throughout the body in the bloodstream and brain, and binds a multitude of diverse cell types. In the periphery, leptin's targets include pancreatic beta cells (modulates insulin production), intestinal enterocytes (pro-angiogenic and reduced glucose absorption), vascular endothelial cells (modulates extracellular matrix), and immune cells including macrophages and T-cells (pro-inflammatory) (Cammisotto et al., 2005; Muoio & Lynis Dohm, 2002). In ARC AgRP neurons, leptin binds its cognate receptor leptin receptor (LepRb), previously referred to as ObR or obesity receptor. LepR is a type I cytokine receptor and specifically part of the interleukin 6 (IL-6) receptor family which contains the glycoprotein 130 (gp130) subunit. Several isoforms of LepR have been described, but all share the same extracellular cytokine receptor homology-2 (CRH2) domain which is required for leptin binding (Iserentant et al., 2005; Zabeau et al., 2012). The mechanisms underpinning leptin-dependent changes of membrane excitability of ARC neurons is discussed in the next section in more detail.

Electrophysiology of ARC and SCN neurons

VIP, cell autonomous firing, and synchrony of pacemaker activity in the SCN

Neurons in both the SCN and ARC have properties of pacemaker cells, exhibiting rhythmic firing patterns during their periods of increased activity (Herzog et al., 2017). When active, SCN neurons fire action potentials at short, regular intervals, and the frequency of these outputs provides direct information about the time of day to downstream brain regions. Neuronal activity in the SCN neurons is directly linked to TTFLs, and changes in electrical activity are coupled to oscillations in the concentration of transcription factors. During the light phase, spontaneous activity of SCN neurons gradually increases, peaking around early morning. Conversely, SCN neurons fire slowly during the dark phase, reaching a nadir in the early night. This phenomenon is driven by diurnal modulation of ion conductances which are phase locked with Per2 expression (Atkinson et al., 2011). In the daytime, the increased intrinsic excitability of SCN neurons is conferred by rising sodium (Na+) conductances. Conversely, during the dark phase, increases in K+ conductance drives inhibition of spontaneous firing. In both cases, changes are driven by regulation of ion channels. In the quiet phase, BK channels are active and mediate an inhibitory potassium current referred to as K+ drag. Inactivation of these BK channels increases the excitability of SCN neurons during light phase (Whitt et al., 2016).

ARC neurons exhibit TTFLs and circadian oscillations in firing

Meal timing is an essential behavior in mammals, where temporal coordination of rest and food consumption are critical for survival. Thus, it is unsurprising that ARC neurons exhibit properties of circadian rhythmicity, exhibiting daily oscillations of TTFLs and spontaneous firing. Per2:Luciferase imaging of the ARC and basomedial hypothalamus demonstrates ARC neurons have circadian oscillations with roughly 24 hour periods that peak in the early night (Guilding et al., 2009). Bioluminescence of Per2 oscillations are observed most strongly in dorsal ARC cells that line the ventricle and less prominently (although still detectable) in lateral ARC cells (Guilding et al., 2009). Concomitantly, ARC cells exhibit circadian rhythmicity in firing rate, and spontaneous firing of AgRP neurons is highest in early evening during the start of dark phase, when mice are typically active and seeking food. For instance, Mandelblat-Cerf et. al. used *in vivo* optrode to measure the activity of AgRP neurons throughout the light cycle and found that the firing rate and number of short interspike intervals is fewer in the morning (1.4 ± 0.3 Hz) and greater in the afternoon (7.6 ± 1.7 Hz) (Mandelblat-Cerf et al., 2015). Although these results support that AgRP and ARC neurons may function as an extra-SCN endogenous clock, SCN inputs to AgRP probably drive much of the rhythmicity in intact animals, as oscillations in ARC explants dampen quickly and exhibit much smaller amplitudes *in vitro* compared to SCN explants (Guilding et al., 2009).

Peripheral inputs mediate AgRP neuron silencing during nutrient presentation, consumption, and absorption

In addition to circadian linked changes in spontaneous activity, the firing rate of AgRP neurons declines over different time courses in response to peripheral inputs signaling food seeking, consumption, and energy balance. Even before food is consumed, exposure to sensory cues indicating food availability causes rapid, temporary reductions in spontaneous firing of AgRP neurons within seconds (Berrios et al., 2021; Y. Chen et al., 2015). After consuming food, sensory neurons in the gut detect the presence of macronutrients such as fats and sugars, and relay this information to the hypothalamus via spinal afferents and vagal nerve transmission (Alhadeff et al., 2019; Borgmann et al., 2021). These gastric inputs subsequently drive stronger, longer lasting silencing of AgRP neurons and are observed to occur within minutes of intragastric infusions of nutrients (Beutler et al., 2017; Su et al., 2017). Finally, as nutrients are absorbed and animals reach a state of energy equilibrium, AgRP neurons undergo further and even more persistent silencing in response to secreted factors such as leptin and insulin (Beutler et al., 2017). Conversely, during states of energy deficiency, the firing rate of AgRP neurons activity is highest (Takahashi & Cone, 2005). This phenomenon is mediated in part by the orexigenic peptide ghrelin, a hormone released by enteric cells in the gut, which is most abundant in the circulation before meals or after periods of fasting. The mechanisms underlying ghrelin's stimulation of hunger and increases in AgRP activity has been a subject of debate (Andrews et al., 2008), as neurons expressing growth hormone secretagogue receptor (GHS-R), ghrelin's cognate receptor, are observed throughout the brain. Furthermore, experiments demonstrated intracranial infusions of ghrelin to multiple

brain regions can drive food intake (Müller et al., 2015). AgRP neurons express high levels GHS-R, which is partially responsible for the direct activation of AgRP neurons in response to ghrelin secretion (Andrews et al., 2008; Dietrich et al., 2010).

Findings from patch clamp electrophysiology recordings in AgRP neurons

Parallel findings from patch clamp electrophysiology of AgRP neurons selectively expressing ChR2 in acute brain slices showed that increasing the frequency of stimulation of afferents results in increasing GABAergic inhibition of innervated cells in downstream regions, such as the PVH (Atasoy et. al. 2012). Remarkably, in this same experiment Atasoy et. al. found that a single 1ms light pulse was capable of producing an increase of IPSCs that could last up to 1s. Also notable was the finding that the strength of the GABAergic input (i.e. the amount of GABA being released and subsequent PVH inhibition) increased with successive stimulations and reached a higher steady state later for 10 Hz vs 5 Hz stimulation paradigms (Atasoy et. al. 2012). Thus, with regard to the goal of faithfully replicating the endogenous outputs during in vivo or in vitro experiments, low frequency stimulation may best recapitulate the natural system, because a single action potential from an AgRP neuron can have ionotropically mediated GABAergic effects that last several orders of magnitude longer than the action potential itself (Atasoy et. al. 2012). Twenty Hz (10ms pulses) of 12–18 mW light appears to be the highest frequency tested in optogenetic experiments on AgPR neurons (Chen et al. 2019). It should be noted most of these experiments were performed during daytime portions of animal light cycles, when AgRP neuron firing is generally thought to be relatively low, which is discussed in the next section.

Effects of leptin on membrane excitability of ARC neurons

Leptin mediated inhibition of ARC neurons is well established, and AgRP neurons undergo a reduction in membrane potential and spontaneous firing after leptin application during patch clamp electrophysiology experiments (Baver et al., 2014; Takahashi & Cone, 2005). However, the mechanism underlying this phenomenon eluded scientists for decades. The earliest studies examining the mechanism driving leptin based inhibition of ARC neurons pointed to changes in K+ conductance as the primary driver of this reduction in excitability. This work implicated ATP sensitive potassium channels as the major ionotropic mediator of these events (Spanswick et al., 1997, 2000). These studies lacked specificity for AgRP and POMC cell types and were associated with glucose responsive cells in the arcuate (Spanswick et al., 1997, 2000). Studies have since characterized the mechanisms by which LepRb and other receptor mediated intracellular signaling can modulate ionotropic receptors in ARC neurons (Bermeo et al., 2020; Y. Gao et al., 2017; J. W. Hill et al., 2008; Qiu et al., 2010; M. A. Smith et al., 2018; Spanswick et al., 1997, 2000; van den Top et al., 2004; J.-H. Wang et al., 2008; Yang et al., 2010). In ARC AgRP neurons, leptin's inhibitory effects are at least partially mediated by activation of ATP-sensitive inward rectifier potassium (ATP-K) and large-conductance Ca2+-activated potassium (BK) channels (van den Top et al. 2004; Yang et al. 2010). The role that leptin's major second messenger phosphoinositide 3-kinase (PI3K) plays in regulation of these ionotropic receptors has been debated (Lee et al. 2018), but leptin inhibition in ARC AgRP neurons likely involves signaling through AMP-activated protein kinase (AMPK) mediated inhibition of L-type calcium conductance (Minokoshi et al. 2004; Bermeo et al. 2020). Inhibition of AgRP neurons by leptin is notably distinct from leptin-

based activation of POMC neurons (Wang et al. 2008), which is mediated by PI3K signaling (Hill et al. 2008), via a combination of transient receptor potential channel 5 (Trpc5) activation (Qiu et al. 2010; Gao et al. 2017) and activation of R-type calcium conductance through regulation of voltage-dependent R-type calcium channel subunit alpha-1E (CaV2.3) (Smith et al. 2018).

Chapter 2
Drd1-signaling Decreases the Firing Rate of SCN Neurons

Summary

Obesity is a pandemic driven by the consumption of high calorie foods. Besides aberrant weight gain and resultant negative health and economic impacts of obesity, Grippo et. al. 2020 and others have presented evidence that high fat, high sugar diet (HFD) results in mismanagement of meal timing and dampened circadian rhythmicity (Chaix et al., 2021; Grippo et al., 2020). The work presented here includes a subset of the experiments performed in Grippo et. al. 2020 and focuses on the patch clamp electrophysiology studies of SCN using CRACM and the selective Drd1 agonist SKF-81279.

Introduction

Studying DA in the SCN and the impact of HFD on circadian rhythmicity is vital to understanding the impact of hedonic systems on homeostatic processes. In the mouse, the suprachiasmatic nucleus (SCN) contains approximately 20,000 neurons which fire during the daytime and are quiescent during the night (Herzog et al., 2017). The SCN acts as the master central clock and outputs from the SCN control phasic behavioral activity or circadian rhythms in diurnal and nocturnal mammalian species (Weaver, 1998). Neural activity of the SCN is necessary for proper timing of essential behaviors including

sleeping, locomotion, feeding, and drinking (Aalto & Kiianmaa, 1984). The phase of the SCN's activity is regulated by several environmental cues known as *Zeitgebers* (German: time giver), the most potent of which is light. However, non-photic *Zeitgebers* influence the clock's phase (Hastings et al., 1997), including exercise (Hastings et al., 1997; C.-Y. Wang, 2017), feeding (Grippo et al., 2020), social interactions (Hastings et al., 1997; Mrosovsky et al., 1989), and temperature (Okamoto-Mizuno & Mizuno, 2012). The SCN's rhythmic activity is maintained through cyclic synthesis and degradation of several transcription factors, including Per1/Per2 and CLOCK/BMAL1, which form transcription translation feedback loops (TTFLs) (Weaver, 1998). Photic input can modulate TTFLs through metabotropic signals passed to the SCN from the retinohypothalamic pathway (LeSauter et al., 2011). Disruption of the Per1/Per2 and CLOCK/BMAL1 TTFLs can result in a variety of disease states including obesity and altered immune function (West & Bechtold, 2015)

SCN neurons expressing vasoactive intestinal peptide (VIP) and/or its cognate receptor VIP receptor 2 (Vipr2, sometimes VPAC2) are necessary for normal detection and entrainment to light (Hermanstyne et al., 2016). Vipr2 is a type 2 G protein-coupled receptor (GPCR), which signals through activation/stimulation of adenylyl cyclase (Ga/s) and second messengers including cyclic adenosine monophosphate (cAMP) and protein kinase A (PKA) (Atkinson et al., 2011). VIP neurons receive excitatory inputs from the intrinsically photoreceptive retinal ganglion cells whose axons constitute the retinohypothalamic tract. Upon activation, SCN VIP neurons secrete VIP onto surrounding neurons (Varadarajan et al., 2018). SCN VIP signaling acts to synchronize

the individual firing rates and TTFL's of local SCN neurons, which can oscillate independently in the absence of such inputs (Herzog et al., 2017). While the role of VIP signaling in circadian biology has been well documented, the influence of other Ga/s type receptor signaling in the SCN is not as well established. For instance, evidence suggests that dopamine 1 receptor (Drd1) may be another type 2 GPCR present in SCN neurons (Jones et al., 2015; Missale et al., 1998; Smyllie et al., 2016), although its influence on the neural activity and TTFLs of the SCN is poorly understood.

While the discrete mechanisms of dopamine signaling in the SCN have thus far evaded scientists, monoaminergic signaling in the brain is known to be essential to sleep and feeding behaviors (Hastings et al., 1997; Varadarajan et al., 2018). DA and its cognate receptors (dopamine receptors 1-5, i.e. DARs, e.g., Drd1) are essential players in neural processes of learning, attention, and reward (Beaulieu & Gainetdinov, 2011; Missale et al., 1998). DA has traditionally been associated with hedonic systems of pleasure and reinforcement, but now our understanding of DA's influence in homeostatic systems is growing (Wise, 2006). For instance, Drd1 neurons in the nucleus accumbens control animal arousal during wakefulness (Y.-J. Luo et al., 2018), and hypothalamic dopamine signaling is known to influence homeostatic processes such as feeding (Alhadeff et al., 2019; Grippo et al., 2020; Mazzone et al., 2020) and mating (S. X. Zhang et al., 2021). Additionally, drugs of abuse such as ethanol, amphetamines, and cocaine, which are well established modulators of DA processes, have profound effects on circadian rhythmicity (Cahill et al., 2014; Paulson et al., 1991). Drd1 has been localized to SCN neurons in primates (Rivkees & Lachowicz, 1997), and Grippo et. al. identified projections of

dopamine neurons located in the midbrain ventral tegmental area (VTA) to the SCN (Grippo et al., 2017). These results, coupled with the observation that VIPR2 and Drd1 share the same Ga/s signaling pathway, make Drd1-dependent signaling a promising mechanism through which drugs and rewarding stimuli may influence neural activity in the SCN.

To investigate the role of Drd1 in the SCN, we incubated acute coronal SCN brain slices in artificial cerebrospinal fluid (ACSF) containing the selective Drd1 agonist SKF 81297 (SKF) and performed patch clamp electrophysiology to measure differences in spontaneous firing. We found that SKF 81297 significantly decreased neuronal firing across day and night conditions in the SCN of wild type mice, but not the SCN of mice null for Drd1. We used Channelrhodopsin assisted circuit mapping (CRACM) (Petreanu et al., 2007) to identify connections between SCN Drd1 neurons and other SCN cells and find local GABAergic signaling plays an important role in Drd1-dependent inhibition. These results provide novel functional evidence of Drd1 signaling in SCN neurons and suggest SCN Drd1 neurons form a local inhibitory microcircuitry. In the context of Grippo et. al. 2020, these findings highlight one possible mechanism by which a high fat diet can disrupt proper meal timing and dampen circadian rhythms.

Results and Figures

Figure 1: SCN neurons can be inhibited in a Drd1-dependent manner

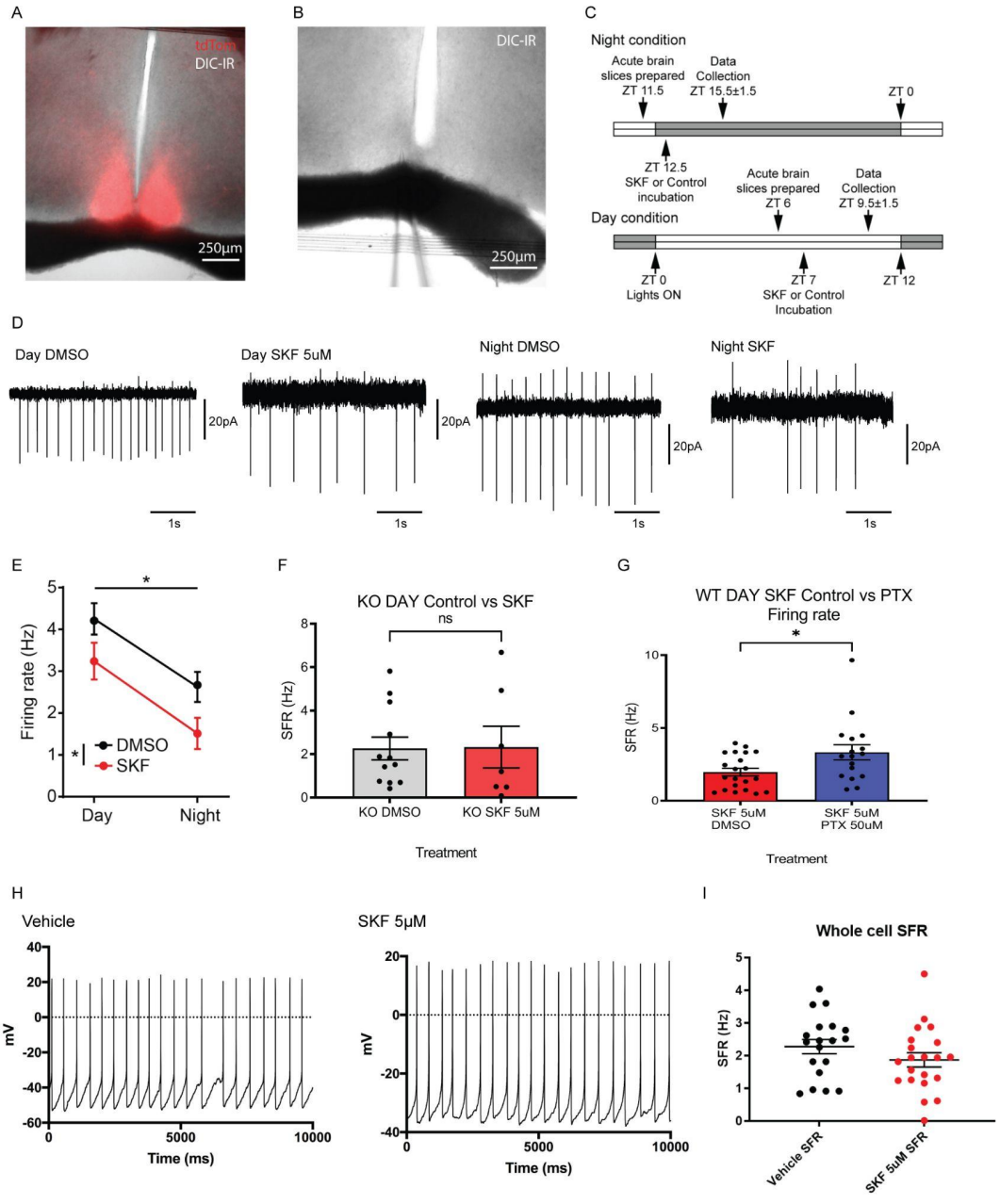

Figure 1 Legend

A. Presence of 40x DIC IR and fluorescence of Drd1-Tdtom in SCN acute coronal brain slices.
B. Representative image of 40x DIC IR WT SCN acute coronal brain slices used in incubation experiments described in Figure 1C-G
C. Diagram of experimental setup of SKF incubation
D. Representative cell attached traces for SCN neuron recordings following SKF-81297 (5 μM) of vehicle incubation at ZT8–ZT11 (day) or ZT14–ZT17 (night).
E. Mean firing rate of cell-attached SCN neuron recordings following SKF-81297 (5 μM) incubation at ZT8–ZT11 (day) or ZT14–ZT17 (night). Two-way ANOVA; n = 13–26/group; $F_{time}(1,70) = 16.9$, $p < 0.001$; $F_{treatment}(1,70) = 6.8$, $p = 0.01$.
F. Mean firing rate and individual values for cell attached KO animal SCN neuron recordings, following SKF-81297 (5 μM) incubation at ZT8–ZT11 (day). Student's two tailed paired t-test, n=7-12/group. Data are represented as mean ± SEM, *p<0.05,**p<0.01,***p<0.001.
G. Mean firing rate and individual values for cell attached WT SCN neuron recordings, following SKF-81297 (5 μM) incubation at ZT8–ZT11 (day) with PTX (50 μM) or vehicle
H. Representative traces of whole cell current clamp recordings of neurons SCN neuron recordings following SKF-81297 (5 μM) or vehicle incubation at ZT8–ZT11 (day)

I. Mean firing rate and individual values of whole cell current clamp recordings of neurons SCN neuron recordings following SKF-81297 (5 μM) or vehicle incubation at ZT8–ZT11 (day)

Results: SCN neurons can be inhibited in a Drd1-dependent manner following incubation with Drd1 agonist SKF

To visualize SCN^{Drd1+}, we crossed $Drd1^{tm1(cre)Rpa}$ (i.e. Drd1-Cre) mice (Heusner et al., 2008) with $Gt(ROSA)26Sor^{tm9(CAG-tdTomato)Hze}$ (i.e. Ai9 or TdTomato) mice (Madisen et al., 2010), generating $Drd1^{(cre/+)}$;$tdTomato^{(td/+)}$ double transgenic mice, which express TdTomato when Cre recombinase is expressed from the Drd1a locus. Similar to Grippo et. al. 2017, we observed tdTomato fluorescence throughout the SCN in acute coronal brain slices of the SCN, confirming functional Cre expression (Figure 1A). Previous studies in using Drd1-Cre mice have validated Drd1a-promoter-driven Cre expression in the SCN of adult animals (Grippo et al., 2017). Grippo et. al. 2020 show that HFD induces increased SCN DA turnover, but failed to observe changes in circadian gene expression, so we sought to evaluate the impact of increased Drd1 signaling on neuronal activity within the SCN. To accomplish this, we incubated acute brain slices from WT mice with the selective Drd1 agonist (SKF-81279; 5 μM) and performed loose cell-attached recordings on randomly selected SCN neurons at ZT8–ZT11 (day) and ZT14–ZT17 (night). Incubation with SKF-81297 significantly decreased the firing rate of neurons within the SCN during both phases (day: DMSO 4.3 ± 0.4 Hz; day: SKF 3.2 ± 0.4 Hz; night: DMSO 2.6 ± 0.4 Hz; night: SKF 1.5 ± 0.4 Hz; Figures 1D and 1E). To further confirm the

observed changes in firing rate were Drd1-dependent, we repeated day incubation experiments in Drd1$^{(cre/cre)}$ knockout (KO) mice, which lack WT Drd1a alleles and instead express Cre recombinase at the Drd1a locus, resulting in animals previously shown to be incapable of functional Drd1-signaling (Grippo et al., 2020). Cell attached recordings in KO animals showed no differences in firing rate between vehicle and SKF incubation in the daytime condition (Figure 1F), further confirming functional Drd1 signaling. Because the majority of SCN neurons are GABAergic, we asked if Drd1 signaling could be inhibiting SCN neurons through a local GABAergic microcircuit. We repeated day SKF experiments in WT animals, with the inclusion of the GABA receptor blocker picrotoxin (PTX). Cell attached recordings in SKF/PTX incubated slices resulted in significantly faster firing rate of day SCN neurons (Figure 1G), suggesting a role for GABAergic signaling in Drd1-dependent inhibition of SCN neurons. To further investigate the effects of Drd1 signaling on membrane properties of SCN neurons, we repeated day SKF experiments in WT animals and performed whole cell current clamp recordings (Figures 1H and 1I). As previously reported by others, we observed the firing rate in our whole cell recordings was lower than the firing rate observed in our cell attached recordings in the day condition (Atkinson et al., 2011). We did not observe significant differences in firing rate in day SKF neurons. We speculate this may be in part due to dialysis of intracellular spaces with the patch pipette solution and rundown of ionotropic processes in SCN cells (Cloues & Sather, 2003). The difficulties associated with obtaining an accurate measurements of firing rate in whole cell recordings of SCN neurons have been previously reported (Cloues & Sather, 2003; J. Fan et al., 2015; Hermanstyne et al., 2016; Schaap et al., 1999). Additionally, we were unable to reliably observe acute effects of the

agonist in whole cell recordings of WT SCN neurons on a time scale of minutes, despite validating the acute effects of SKF on medium spiny neurons in our hands as reported previously (Hernández-López et al., 1997), see discussion. Taken together our results support Drd1-dependent inhibition of SCN neurons on a time scale of hours.

Figure 2: SCN^{Drd1+} neurons possess GABAergic outputs to other SCN neurons

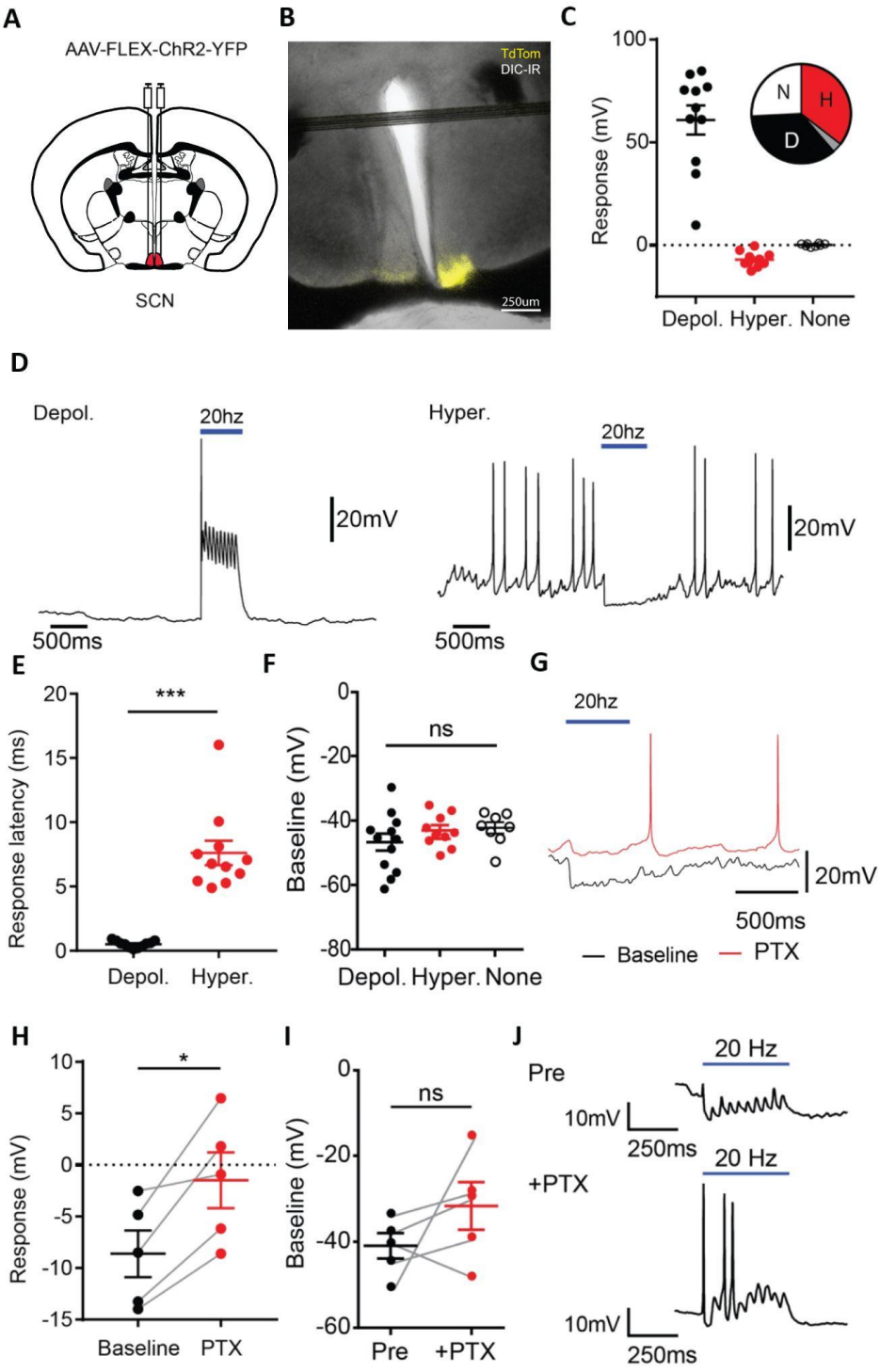

Figure 2 Legend

A. Schematic of bilateral intracranial injection of Cre dependent ChR2-YFP to the SCN of Drd1-Cre mice.
B. Representative image of 40x DIC IR and fluorescence of ChR2-YFP SCN viral expression in acute coronal brain slices.
C. ChR2 stimulation-induced average peak responses for depolarizing (depol.), hyperpolarizing (hyper.), and non-responsive (none) neurons. Distribution of recorded responses is depicted
D. Representative whole cell current clamp traces of neuron responses to a 500 ms train of 20 Hz 10 ms pulses of light, for ChR2+ (left) and hyperpolarizing (right) neurons, respectively
E. Response latency of each group in (D). Student's two-tailed t test; n = 11/group.
F. Baseline membrane potential of three types of neurons described in (Figure 2C) before light stimulation. One-way ANOVA, n=8-12/group.
G. Representative traces from whole-cell current-clamp recordings for ChR2 stimulation-induced postsynaptic responses before and after 5-min 100 μM PTX incubation.
H. ChR2 stimulation-induced average peak responses before and after PTX incubation. Student's two-tailed paired t test; n = 5/group.
I. Baseline membrane potential of neurons that hyperpolarize in response to ChR2 stimulation, before (Pre) or after picrotoxin incubation (+PTX). Student's two tailed paired t-test, n=5/group. Data are represented as mean ± SEM, *p<0.05,**p<0.01,***p<0.001.

J. Example trace for one SCN neuron that has both hyperpolarizing and depolarizing response to light stimulation from Figure 2I. Top: Before picrotoxin incubation (Pre), the light stimulation induces hyperpolarization with re-occurring depolarization events time locked to each light pulse without exhibiting action potentials. Bottom: Following incubation of picrotoxin (+PTX), action potential light stimulation evokes action potentials.

Results: SCNDrd1+ neurons possess GABAergic outputs to other SCN neurons

Drd1 is a Gs-coupled GPCR, and the majority if not all of SCN neurons are GABAergic (R. Y. Moore & Speh, 1993; Okamura et al., 1989). Work by Grippo et. al. 2020 confirmed the presence of glutamate decarboxylase (GAD), the principal enzyme in GABA synthesis, in SCN neurons (Grippo et al., 2020). These observations, coupled with our finding that PTX increases SCN neuron firing during Drd1-dependent inhibition (Figure 1G) led us to hypothesize that stimulation of Drd1-expressing SCN neurons attenuates the overall firing rate of the local microcircuitry. Therefore, we performed whole-cell current clamp recordings from the SCN of $Drd1^{(Cre/+)}$ mice injected with an AAV2 that expresses ChR2 Cre-dependently (AAV2-DIO-ChR2-YFP; Figure 2B). Neurons were randomly selected during electrophysiological recordings independent of ChR2 expression within the anatomically defined region of the SCN. Although 26% of recorded cells (8 cells) had no response to light stimulation, 35% of the cells depolarized within 1 to 2 ms of the stimulation with time-locked optogenetic responses indicative of ChR2

expression in these cells (11 cells). Additionally, 35% of the SCN neurons hyperpolarized following a minimum of 4-ms delay (11 cells; Figures 2C-2F), although one neuron displayed both light-induced action potentials and post-stimulation hyperpolarization (Figure 2J). Perfusion picrotoxin (PTX) (100 μM), diminished the amplitude of the inhibitory responses, confirming that they are ChR2-driven postsynaptic currents (Figures 2G and 2H). These data identify a local inhibitory response to Drd1-SCN neuron activation, revealing that the HFD-induced elevated DA tone observed in Grippo et. al. 2020 may directly modulate SCN firing rate (Grippo et al., 2020).

Discussion

DA system as a novel target for circadian related sleep disorders and obesity

Grippo et. al. 2020 showed that a high fat and sugar diet results in increased dopamine signaling in the SCN and mis-timing of feeding. Previous work showed that striatal D2R, the Gi coupled DA receptor class, plays a role in addiction and compulsive eating processes, and reducing D2R signaling accelerates addiction progression and weight gain from high calorie diets (Johnson & Kenny, 2010). Our results suggest that DA input to the SCN from rewarding foods leads to a Drd1-dependent reduction in neuronal activity of the SCN, and contributes to the dampening of SCN rhythmicity. Snacking and meal consumption outside of regular times can have negative consequences for animals and leads to increased weight gain and obesity in mice (Grippo et al., 2020). Conversely, time restricted feeding (TFR) has been shown to have protective effects in mice, including prevention of fatty liver, preservation of glucose regulation, and better outcomes during

sepsis, although some of these effects are sex and age dependent (Chaix et al., 2021). Thus, DA inputs to the SCN during consumption of rewarding food represents a novel therapeutic target in the treatment of sleep disorders and obesity. Future studies will identify how SCN dampening increases food consumption and determine how outputs from SCN neurons impact activity in orexigenic nuclei in the hypothalamus.

GABAergic microcircuitry of the SCN

The connectivity of the SCN has been characterized according to molecular markers and proteins expressed by SCN cells, including VIP, arginine vasopressin (AVP), (enkephalin) ENK, gastrin-releasing peptide (GRP), calretinin (CALR) (Varadarajan et al., 2018), and neuromedin S (NMS) (Smyllie et al., 2016). Our work adds to this growing body of knowledge and provides evidence for functional Drd1 expression in the SCN. In normal 12hr light/12hr dark cycles, VIP-signaling from neurons at the base of the SCN synchronize and activate other SCN neurons, including AVP neurons in the dorsomedial SCN (Abrahamson & Moore, 2001; Robert Y. Moore et al., 2002). SCN neurons are predominantly GABAergic (R. Y. Moore & Speh, 1993; Okamura et al., 1989), and our work provides more evidence that SCN neurons possess GABAergic interconnections. Because we randomly selected SCN neurons for patching, we cannot know the exact connectivity of the neurons in this work, and thus additional experiments are needed to elucidate the exact connectivity of the Drd1 neurons in the SCN. Based on our CRACM experiments and our observation that PTX can counteract SKF driven reduction in firing rates, we posit that Drd1-signaling results in increased GABAergic tone in the SCN, driving the observed decrease in activity. Elucidating the projection patterns and connectivity of Drd1 neurons in the SCN would help confirm this hypothesis, and future

experiments should attempt to describe the connections between these neurons. This could be accomplished through visualization of cell type specific labeling of synaptic processes, in conjunction with fluorescent labeling of other neuronal markers. For instance, observations that Drd1:Cre ChR2-mCherry axons synapse exclusively onto AVP, VIP or other SCN cell types would enhance our understanding of these microcircuits.

VIP and DA signaling in the SCN

The firing rate and pacemaker activity of SCN neurons is mediated by rhythmic expression and modulation of ionotropic receptors, including diurnal changes in potassium, sodium, and calcium channel conductances (Jackson et al., 2004; Whitt et al., 2016). VIP is mainly released by cells in a region in the ventral retinorecipient aspect of the SCN, and VPAC2 signaling in SCN neurons drives changes in ionotropic receptors, TTFL phase, and synchronization of individual neurons (Patton et al., 2020). Because the SCN network is densely interconnected, both directly and indirectly, pharmacological experiments looking at acute changes in brain slices are difficult to interpret. Studies using dissociated cultures have proved useful in looking at the effects of peptidergic signaling in SCN neurons (Mazuski et al., 2018), but patch clamp studies of VIP SCN neurons have only been able to show changes in firing rates and membrane potentials on the order of hours (Kudo et al., 2013). Our results regarding the effects of SKF must be taken in the context of the time course of our experiments (hours) and possibly reflect signaling from VIP or other neurons in a pattern different from the canonical VIP-VPAC2 axis (Patton et al., 2020). Other studies have utilized calcium imaging as a method to ascertain topological and spatiotemporal relationships between different parts of the SCN network

(Patton et al., 2020), and future experiments will look at Drd1 signaling using these methods. Overlap between NMS and Drd1 SCN populations is high but not 100%, and questions about the heterogeneity of different SCN markers remain (Smyllie et al., 2016). Grippo et. al. 2020 observe Drd1 expression in both the shell and dorsal regions of the SCN, and future studies will further define subpopulations of neurons which express Drd1 and other markers.

Future work will map SCN outputs to orexigenic circuits

Here in conjunction with the work in Grippo et. al. 2020 we show that HFD results in increased DA tone in the SCN and dampening of circadian behavioral rhythms. Mice consume food during their active phase at night (Mistlberger, 2011), and we posit that dampening of SCN outputs results in weaker outputs from the central circadian nucleus to orexigenic circuits in the brain. SCN neurons possess outputs to other hypothalamic nuclei (Kalsbeek et al., 2006), and the most obvious candidate for SCN modulation of downstream orexigenic processes would be a direct reduction in GABAergic outputs to agouti related peptide (AgRP) neurons in the arcuate nucleus of the hypothalamus (ARC). AgRP neurons display circadian features of firing rate time locked to the phase of SCN neuronal activity (Z. Chen, 2019), and disinhibition of AgRP neurons during daytime would explain the mis-timing of feeding. Future studies will map SCN outputs to orexigenic nuclei in the hypothalamus and further our understanding of circadian dysregulation and obesity.

Methods

Experimental Model and Subject Details

All animal experiments were conducted in compliance with the University of Virginia Institutional Animal Care and Use Committee (IACUC). Animals were provided cotton nesting material (Ancare, Bellmore, NY) and animal cages were individually ventilated and temperature and humidity controlled, (approx. 40% humidity, 22°C–24°C). Animals were housed on a 12 hour light/dark cycle, and given water and food ad libitum, except for approved periods of time during fasting experiments. The following mouse lines were used: Drd1$^{tm1(cre)Rpa}$ (Heusner et al., 2008) and Gt(ROSA)26Sor$^{tm9(CAG-tdTomato)Hze}$, (Madisen et al., 2010). Drd1$^{(Cre/Cre)}$ (KO) mice and littermates bred for husbandry were raised on standard chow diet of Teklad 8664 (Envigo, United Kingdom) or PicoLab Rodent Diet 20 5053 (LabDiet, USA) placed on the cage floor to facilitate access to the food for the Drd1-KO mice.

Methods Details

Mouse diets

Standard chow diet (SCD):Teklad 8664 (Envigo, United Kingdom: 3.1 kcal/gram; 19% fat, 31% protein, 50% carbohydrates) or PicoLab Rodent Diet 20 5053 (3.07 kcal/gram; 13% fat, 24% protein, 62% carbohydrates; 3.2% sucrose).

Viral Expression and Stereotaxic Surgery

All surgery was performed on mice between 8 and 14 weeks of age using aseptic technique in compliance with the University of Virginia IACUC. Surgical anesthesia was induced with 5% isoflurane (Isothesia) and then maintained at 2% to 2.5% throughout the procedure. After induction animals were mounted in a stereotaxic frame (Kopf) with an electric heating pad underneath to maintain body temperature. Veterinary ocular lubricant was used on each animal's eyes and reapplied as necessary to prevent dehydration/desiccation. A recombinant AAV was used to express a specific transgene, containing a double-floxed inverted open reading frame (DIO cassette). Virus was delivered at 100nl/min by a microsyringe pump controller (World Precision Instruments, model Micro 4), via a 10 µL syringe (Hamilton) and 26-gauge needle (Hamilton). After infusion of the AAV was completed, the syringe was left in place for 10 min, after which it was retracted 0.2mm and then left in place for another 10 minutes before being withdrawn completely. As an analgesic, immediately after surgery mice and for three days post surgery mice were subcutaneously injected with veterinary ibuprofen (ketoprofen, 3 mg/kg).

Viral constructs

AAV1-hSyn-DIO-ChR2(H134R)-eYFP (500 nl; 6.9 × 10ˆ11 viral genomes/ul) was injected into the SCN (ML: ± 0.28 mm, AP: - 0.30 mm, DV: −5.75 mm). All coordinates are relative to bregma (George Paxinos and Keith B. J. Franklin).

Slice electrophysiology

Slice visualization and data collection: SCN cells were visualized with infrared DIC in an upright Slicescope 6000 microscope. The SCN was identified by the shape of the both 3rd ventricle and most inferior middle region of the slice, as well as the presence of the optic chiasm. Images of patched brain regions were taken using Scientifica SciPro camera and Ocular imaging software. A Multiclamp 700B amplifier and Digidata 1550B digitizer (Molecular Devices; San Jose, California) were used to perform all patch clamp experiments. All experiments were conducted using 2.5-6MΩ microelectrodes pulled with a Sutter P97 puller. All brain slice solutions were saturated with 95% O2 and 5% CO2 gas. SKF-81297 was used at 5 μM concentration in all incubation experiments.

Cell attached recordings: Male and female WT mice were individually housed in light-tight boxes under a 12 hr:12 hr LD cycle for at least 7 days. Mice between P31 and P55 were deeply anesthetized with isoflurane and brains were rapidly dissected and mounted for slicing in the compresstome slicer. Slices were taken with in ice cold HEPES based holding ACSF solution containing (in mM): 92 NaCl, 2.5 KCl, 1.25 NaH2PO4, 30 NaHCO3, 20 HEPES, 25 glucose, 2 thiourea, 5 Na-ascorbate, 3 Na-pyruvate, 2 CaCl2·4H2O and 2 MgSO4·7H2O with pH ranging from 7.3 to 7.4 and osmolarity ranging from 300 to 310 mOsm (Ting et al., 2014, 2018). Slices were allowed to recover for ≤ 12 min at 34°C in the same HEPES based holding ACSF solution, and then allowed to come to room temperature. ‘Day’ collections condition (sacrificed at ZT 5-6) were incubated for a minimum of 90 min, and data was collected between ZT 8 and 11. ‘Night’ collections condition (sacrificed at ZT 11-12) were incubated and data was collected at ZT 14 to 17.

After a minimum of 90 min of incubation slices were transferred to the microscope recording bath and superfused with a continuous flow (1.5 - 2 ml/min) recording ACSF which consisted of (in mM): 124 NaCl, 2.5 KCl, 1.2 NaH2PO4, 24 NaHCO3, 5 HEPES, 10 glucose, 2 CaCl2·4H2O and 2 MgSO4·7H2O with pH ranging from 7.3 to 7.4 and osmolarity ranging from 300 to 310 mOsm, and included the vehicle or agonist. The resulting DMSO concentration in these buffers ranged from 0.01% to 0.12%. Vehicle control solutions contained the same amount of DMSO as the treatment conditions. Drug solutions were added directly to the bath after the recovery incubation. Cell attached recordings were made at 32°C. For cell attached recordings the pipette was filled with ACSF, slight positive pressure applied when approaching the cell was released and the seal was allowed. Seal magnitude ranged from 5 to 50MΩ. In all experiments the pipette offset was < 15mV, typically ranging from 1 to 11mV. Pipette offset was set just before initiating a recording, and the seal resistance was monitored closely. Recordings measuring spontaneous spiking lasted approximately 1 min. Recordings were filtered offline at 1kHz and baseline was manually adjusted using ClampFit (Molecular devices) software. Action potential events were then extracted using ClampFit and analyzed using custom scripts in MATLAB (Mathworks).

Whole cell recordings and optogenetic stimulation: Whole cell recordings in WT animals were conducted on acute coronal brain slices obtained and treated using the same methods described above for cell attached recordings. All whole cell recordings in WT animals used the same intracellular solution described below used in optogenetic experiments. For optogenetic experiments, heterozygous Drd1$^{(cre/+)}$ mice minimum of 8

weeks of age received bilateral injections of AAV2-DIO-ChR2-YFP to the SCN as previously described. After a minimum of 5 weeks to allow for viral expression and animal recovery, animals were deeply anesthetized (ketamine:xylazine, 280:80 mg/kg, i.p.) and transcardially perfused with an NMDG recovery ACSF solution containing (in mM): 92 NMDG, 2.5 KCl, 1.25 NaH_2PO_4, 30 $NaHCO_3$, 20 HEPES, 25 glucose, 2 thiourea, 5 Na-ascorbate, 3 Na-pyruvate, 0.5 $CaCl_2 \cdot 4H_2O$ and 10 $MgSO_4 \cdot 7H_2O$, pH adjusted to 7.3 to 7.4, osmolarity 300 to 310 mOsm (Ting et al., 2014, 2018). Slices were held in the NMDG recovery ACSF for ≤ 12 min at 34°C, and then transferred to recording ACSF (described above) and allowed to rest at room temperature for 45 min before being transferred to the microscope bath for data collection. All recordings were made at room temperature and a potassium gluconate (K-glu) based intracellular solution containing 135 K-glu, 5 KCl, 5 NaCl, 10 HEPES, 2.5 MgATP, 0.3 GTP, pH 7.2-7.4, 290mOsm (LeSauter et al., 2011). SCN cells were randomly patched without regard for YFP expression. After formation of a gigaohm seal (> 2GΩ), cell membrane was ruptured and current clamp recordings acquired. A minimal current injection hold of 0 to −15pA was used to compensate for minor current leakage. Whole cell voltage measurements made as described for whole cell incubation recordings. Optogenetic stimulation consisted of 500ms of 20 Hz square pulses of 488 nm light (10 pulses total, each pulse 10ms). Light was delivered at the beginning of each 10 s trace. For a subset of cells (5) which showed a hyperpolarized response to blue light stimulation, recording ACSF with 100 μM Picrotoxin (PTX) was perfused for 6 min and cell responses to the optogenetic stimulation protocol were recorded. No further recordings were made on slices which were exposed to PTX.

Response magnitudes and latencies were manually extracted in ClampFit, and consisted of an average of 5-6 traces.

Chapter 3
Arcuate AgRP/NPY-neurons receive local Drd1-neuron input

Authors/affiliations

Sean R. Chadwick [1] and Ali D. Güler *, [1, 2, 3]

Author list footnotes

1 Program in Fundamental Neuroscience and the Department of Biology, University of Virginia, Charlottesville, VA 22904, USA

2 Department of Neuroscience, School of Medicine, University of Virginia, Charlottesville, VA 22903, USA

3 Lead Contact

* Corresponding Author

Contact info

Correspondence: aguler@virginia.edu

Summary

Obesity is a pandemic afflicting more than 300 million people worldwide, driven by the consumption of calorically dense and highly rewarding foods. Dopamine (DA) signaling has been implicated in neural responses to highly palatable nutrients, but the exact mechanisms through which DA impinges upon homeostatic feeding circuits remains unknown. A subpopulation of arcuate (ARC) agouti-related peptide (AgRP)/neuropeptide Y (NPY) ($ARC^{AgRP/NPY+}$) neurons are stimulated by DA through activation of the dopamine 1 receptor (Drd1), suggesting a potential avenue for dopaminergic regulation of food intake circuitry. Using patch clamp electrophysiology, we evaluated the responses of Drd1-expressing (ARC^{Drd1+}) neurons in the arcuate nucleus of the hypothalamus to overnight fasting and leptin. While a portion of ARC^{Drd1+} neurons express AgRP/NPY, as a whole ARC^{Drd1+} neurons were less responsive to caloric deficit than $ARC^{AgRP/NPY+}$ neurons. However, ARC^{Drd1+} neurons reduced their activity in response to the satiety signal leptin, as has been observed for $ARC^{AgRP/NPY+}$ neurons. To identify novel functional connections between ARC^{Drd1+} neurons and other ARC neurons we used Channelrhodopsin Assisted Circuit Mapping (CRACM) and found subgroups of ARC^{Drd1+} neurons that differentially modulate $ARC^{AgRP/NPY+}$ neurons. These findings provide evidence for DA as a key player in hypothalamic circuits that underpin appetite regulation and obesity.

Introduction

Throughout the world, human diets are increasingly composed of high calorie food, a major factor contributing to the obesity pandemic (Kearney 2010; Statovci et al. 2017). Overeating is the primary driver of obesity, and consumption of fat and sugar activates the brain's innate reward systems (Berridge et al. 2010; Verdejo-Román et al. 2017). Obese individuals suffer from a plethora of comorbid conditions including type 2 diabetes, cardiovascular disease, cancer, and metabolic syndrome (Engin 2017; Powell-Wiley et al. 2021; Scully et al. 2020; Bhaskaran et al. 2014), and these conditions significantly reduce lifespan and create an enormous burden on healthcare systems (Cawley and Meyerhoefer 2012). Except for invasive bariatric surgery, current treatments for obesity such as altered diet are inadequate for controlling patient weight, particularly over protracted periods of time (Mann et al. 2007). Elucidation of how reward systems impinge on energy balance circuits is necessary to develop better treatment strategies in the fight against this public health crisis.

Within the central nervous system, the arcuate nucleus of the hypothalamus (ARC) is an essential integrator of peripheral signals that reflect metabolic states (Cone et al. 2001; Dietrich and Horvath 2013; Sternson et al. 2013). Landmark experiments demonstrated that activation of ARC agouti-related peptide (AgRP) neurons, which co-express Neuropeptide Y (NPY) (hereinafter referred to as $ARC^{AgRP/NPY+}$ neurons), is sufficient to invoke voracious feeding, even in sated animals (Aponte et al. 2011; Krashes et al. 2011; Atasoy et al. 2012; Betley et al. 2013). $ARC^{AgRP/NPY+}$ neurons are modulated by hormones and neurotransmitters secreted during states of caloric deficit and surplus (Cone et al.

2001; Aponte et al. 2011; Garfield et al. 2016). For instance, $ARC^{AgRP/NPY+}$ neurons increase their firing in response to orexigenic peptides including ghrelin, orexin, neuromedin B, or gastric releasing hormone (GRH) (Hewson et al. 2002; van den Pol et al. 2009; Kohno and Yada 2012; Mandelblat-Cerf et al. 2015; Cowley et al. 2003; Chen et al. 2017). Conversely, $ARC^{AgRP/NPY+}$ neuron firing is decreased in response to peptide YY, insulin, or leptin (Xu et al. 2005; Takahashi and Cone 2005; Yang et al. 2010; Bouret et al. 2012; Baver et al. 2014; Jones et al. 2019). $ARC^{AgRP/NPY+}$ neurons release gamma-aminobutyric acid (GABA), AgRP, and NPY onto their downstream targets, and these inhibitory outputs drive different aspects of feeding behaviors (Krashes et al. 2013; Atasoy et al. 2012; Betley et al. 2013). Today, $ARC^{AgRP/NPY+}$ neurons are recognized as a crucial orexigenic population in energy homeostasis, but our understanding of the discrete molecular mechanisms governing their activity remains incomplete (Claret et al. 2007; Garfield et al. 2016; Alhadeff et al. 2019; Goldstein et al. 2021).

Current models of food intake circuity lack explanations for how information about the rewarding properties of food is integrated with homeostatic systems, and researchers have hypothesized that dopamine (DA) may be a key player in hedonic regulation of appetite during the consumption of rewarding and highly palatable foods (Wise 2006; Palmiter 2007; Alhadeff et al. 2019; Mazzone et al. 2020). Staining for DA receptors has revealed dopamine 1 receptor (Drd1) immunoreactivity in the ARC, peri-ARC, and median eminence (ME) (Romero-Fernández et al. 2014). However, characterization of ARC neuron subtypes has proven challenging (Vong et al. 2011; Krashes et al. 2011; Campbell et al. 2017), and it is unknown which neuronal populations express Drd1 in this region. Recent studies have demonstrated that DA modulates the activity of ARC neurons (Zhang

and van den Pol 2016; Alhadeff et al. 2019), including AgRP neurons that express Drd1 (Zhang and van den Pol 2016). These results implicate DA signaling as one mechanism through which information about the rewarding properties of drugs and palatable foods integrate into homeostatic circuits.

Using patch clamp electrophysiology, we compared the membrane properties of Drd1-expressing neurons (ARC^{Drd1+}) and $ARC^{AgRP/NPY+}$ neurons. ARC^{Drd1+} neurons exhibited significant inhibitory responses to leptin, although these responses were less drastic than those observed in $ARC^{AgRP/NPY+}$ neurons. Surprisingly, ARC^{Drd1+} neurons membrane properties were not significantly affected by overnight fasting. To gain better insight into the role of ARC^{Drd1+} neurons in ARC circuitry, we used Channelrhodopsin Assisted Circuit Mapping (CRACM) to identify novel connections from ARC^{Drd1+} neurons to other ARC neurons and characterized these inputs. We established that the ARC^{Drd1+} neuron population is heterogeneous and includes a subpopulation of neurons which co-express AgRP and NPY ($ARC^{Drd1+;AgRP/NPY+}$). Ultimately, we uncovered subgroups of ARC^{Drd1+} neurons that either inhibit or excite $ARC^{AgRP/NPY+}$ neurons. These findings reveal a complex circuitry where ARC^{Drd1+} neurons can differentially modulate a key population of orexigenic neurons and further our understanding of DA's role in regulation of appetite.

Results and Figures

Figure 1: Overnight fasting increases spontaneous firing in ARC$^{AgRP/NPY+}$ neurons, but not ARC^{Drd1+} neurons

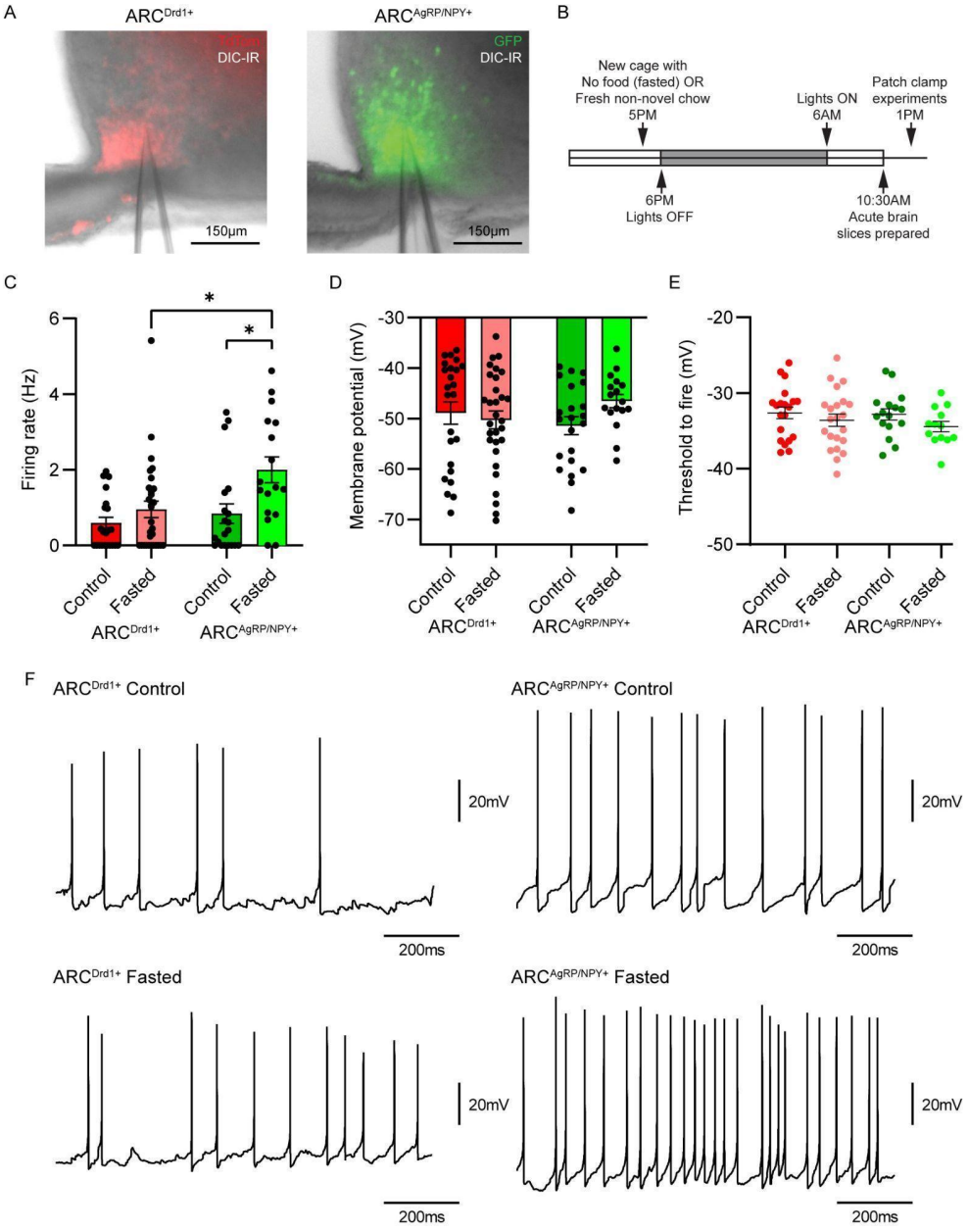

Figure 1 Legend

A. Representative fluorescence images of ARC^{Drd1+} (TdTom, red) and $ARC^{AgRP/NPY+}$ (GFP, green) neurons. Scale bar 150 μM.

B. Diagram of overnight fasting experimental setup.

C. Spontaneous firing rates of ARC^{Drd1+} neurons (n = 24 neurons from control animals and n = 30 neurons from fasted animals) and $ARC^{AgRP/NPY+}$ neurons (n = 20 neurons from control animals and 17 neurons from fasted animals). For all groups: (*p < 0.05, **p < 0.01, ***p < 0.001 as determined by 2-way ANOVA with Bonferroni post-hoc comparison, $F_{genotype}$ (1, 87) = 7.12, p = 0.009; $F_{fasting}$ (1, 87) = 9.73, p = 0.003).

D. Inter spike interval membrane potentials of ARC^{Drd1+} (n = 24 neurons from control animals and n = 30 neurons from fasted animals) and $ARC^{AgRP/NPY+}$ (n = 20 neurons from control animals and 17 neurons from fasted animals). For all groups: (*p < 0.05, **p < 0.01, ***p < 0.001 as determined by 2-way ANOVA with Bonferroni post-hoc comparison, $F_{genotype}$ (1, 87) = 0.104, p = 0.7482; $F_{fasting}$ (1, 87) = 0.830, p = 0.3647).

E. Firing thresholds of ARC^{Drd1+} (n = 20 neurons from control animals and 22 neurons from fasted animals) and $ARC^{AgRP/NPY+}$ (n = 16 neurons from control animals and n = 13 neurons from fasted animals). For all groups: (*p < 0.05, **p < 0.01, ***p < 0.001 as determined by 2-way ANOVA with Bonferroni post-hoc comparison, $F_{genotype}$ (1, 68) = 0.396 p = 0.531; $F_{fasting}$ (1, 68) = 2.42 p = 0.124).

F. Representative traces of whole cell current clamp recordings of spontaneous firing.

Overnight fasting increases spontaneous firing in $ARC^{AgRP/NPY+}$ neurons, but not ARC^{Drd1+} neurons

Drd1 expression has been documented in ARC, including in $ARC^{AgRP/NPY+}$ neurons (Romero-Fernandez et al. 2014; Zhang and van den Pol 2016). However, neurophysiological characteristics of the ARC^{Drd1+} neurons have not been established. Therefore, we determined the electrophysiological properties of ARC^{Drd1+} neurons in comparison to $ARC^{AgRP/NPY+}$ neurons. To visualize Drd1 expressing neurons in the ARC (ARC^{Drd1+}), we crossed $Drd1^{tm1(cre)Rpa}$ (Drd1-Cre) mice (Heusner et al. 2008) with $Gt(ROSA)26Sor^{tm14(CAG-tdTomato)Hze}$ (Ai14 or TdTomato) mice (Madisen et al. 2010), generating $Drd1^{cre/+}$;$tdTomato^{td/+}$ double transgenic animals, which express TdTomato when Cre recombinase is expressed from the *Drd1a* locus. In the hypothalamus, we observed tdTomato expression in the ARC, ME, and ventromedial hypothalamus (VMH) (Figure 1A). To visualize $ARC^{AgRP/NPY+}$ neurons, we used Tg(Npy-hrGFP)1Lowl (NPY-GFP) mice (van den Pol et al. 2009), which express GFP under control of the *Npy* promoter, labeling NPY neurons in the ARC and other brain regions (Figure 1A). To establish the baseline electrical behavior of these two neuronal populations, we performed whole cell current clamp and recorded spontaneous firing in fluorescently labeled ARC^{Drd1+} and $ARC^{AgRP/NPY+}$ neurons from animals provided *ad libitum* access to standard chow (henceforth control ARC^{Drd1+} neurons, and control $ARC^{AgRP/NPY+}$ neurons, respectively) (Figures 1A-D). To further assess membrane excitability, a subset of recorded neurons were injected with progressively increasing steps of square current (Figure 1E). Control ARC^{Drd1+} and $ARC^{AgRP/NPY+}$ neurons did not have significant differences in spontaneous firing rates (ARC^{Drd1+}: 0.60 ± 0.15 Hz; $ARC^{AgRP/NPY+}$: 0.84 ±

0.26 Hz; unpaired two-tailed Student's t-test t = 0.846, df = 42, p = 0.403), inter spike interval membrane potentials (ISI-MPs) (ARC^{Drd1+}: -48.90 ± 2.20 mV; $ARC^{AgRP/NPY+}$: -46.54 ± 1.33 mV ; unpaired two-tailed Student's t-test t = 0.720, df = 43, p = 0.476), and firing thresholds (ARC^{Drd1+}: -32.62 ± 0.77 mV; $ARC^{AgRP/NPY+}$: -32.81 ± 0.75 mV; unpaired two-tailed Student's t-test t = 0.173, df = 34, p = 0.864).

$ARC^{AgRP/NPY+}$ neurons become excited during states of caloric deficiency (Takahashi and Cone 2005; Liu et al. 2012; Wei et al. 2015; Laing et al. 2018), and we hypothesized this phenomenon might also be observable in ARC^{Drd1+} neurons in fasted mice. Therefore, to determine if the electrophysiological properties of ARC^{Drd1+} neurons are impacted by negative energy balance, we fasted $Drd1^{cre/+}$;$tdTomato^{td/+}$ and NPY-GFP mice overnight, and performed whole cell current clamp recordings in fluorescently labeled neurons (Figure 1B). In line with previous reports, $ARC^{AgRP/NPY+}$ neurons from fasted animals (henceforth referred to as fasted $ARC^{AgRP/NPY+}$ neurons) fired at a significantly faster frequency than neurons from control animals (Figure 1C). Strikingly, the spontaneous firing, ISI-MP and firing threshold of ARC^{Drd1+} neurons from fasted animals (fasted ARC^{Drd1+} neurons) were not significantly different from ARC^{Drd1+} neurons from control animals (Figures 1C-E). Additionally, fasted $ARC^{AgRP/NPY+}$ neurons fired at a higher frequency than the ARC^{Drd1+} neurons from fasted mice (Figure 1C). Thus, fasting increases the spontaneous firing rate of $ARC^{AgRP/NPY+}$ neurons, but not ARC^{Drd1+} neurons, indicating that these neuronal populations may not be identical in terms of their inputs or sensitivity to anorexigenic signals.

Figure 2: ARC^{Drd1+} neurons are inhibited by leptin

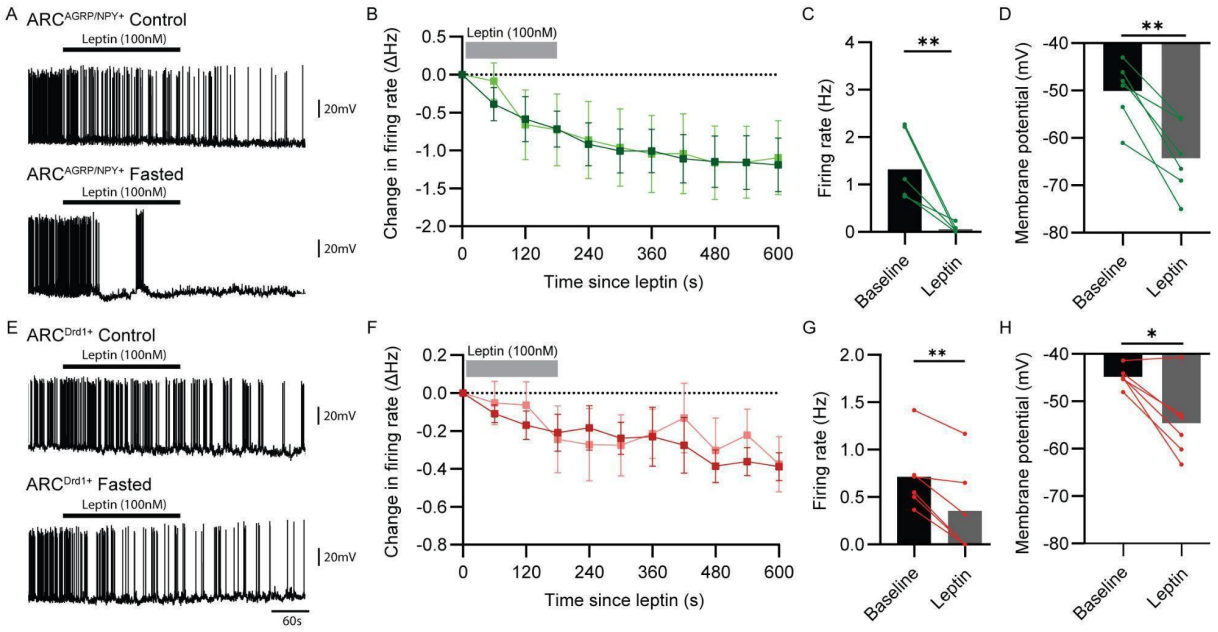

Figure 2 Legend

A. Representative traces of whole cell current clamp recordings of leptin mediated inhibition in ARC$^{AgRP/NPY+}$ neurons from control animals (top) and ARC$^{AgRP/NPY+}$ neurons from fasted animals (bottom).

B. Change in firing rate from baseline for neurons perfused with leptin, binned for 1-minute intervals. Each data point represents the average firing in the previous 60 seconds. Green: control ARC$^{AgRP/NPY+}$ neurons (n = 6); light green: fasted ARC$^{AgRP/NPY+}$ neurons (n = 7). Data are represented as mean ± SEM.

C. Firing rate at baseline and 8 minutes after the start of leptin perfusion for ARC$^{AgRP/NPY+}$ neurons from control animals (*p < 0.05, **p < 0.01, ***p < 0.001 as determined by paired two-tailed Student's t-test, t = 4.14, df = 5, n = 6 pairs).

D. Inter spike interval membrane potential at baseline and 8 minutes after start of leptin perfusion for $ARC^{AgRP/NPY+}$ neurons from control animals (*p < 0.05, **p < 0.01, ***p < 0.001 as determined by paired two-tailed Student's t-test, t = 5.73, df = 5, n = 6 pairs).

E. Representative traces of whole cell current clamp recordings of leptin mediated inhibition in control ARC^{Drd1+} neurons (top) and fasted ARC^{Drd1+} neurons (bottom).

F. Change in firing rate from baseline for neurons perfused with leptin, binned for 1-minute intervals. Each data point represents the average firing in the previous 60 seconds. Red: control ARC^{Drd1+} neurons (n = 6); pink: fasted ARC^{Drd1+} neurons (n = 6). Data are represented as mean ± SEM.

G. Firing rate at baseline and 8 minutes after the start of lepin perfusion for ARC^{Drd1+} neurons from control animals (*p < 0.05, **p < 0.01, ***p < 0.001 as determined by paired two-tailed Student's t-test, t = 4.95, df = 5, n = 6 pairs).

H. Inter spike interval membrane potential at baseline and 8 minutes after start of leptin perfusion for ARC^{Drd1+} neurons from control animals (*p < 0.05, **p < 0.01, ***p < 0.001 as determined by two-tailed Student's t-test, t = 3.81, df = 5, n = 6 pairs).

ARC^{Drd1+} neurons are inhibited by leptin

$ARC^{AgRP/NPY+}$ neurons are inhibited by sensory cues and peripheral signals of food detection, nutrient consumption, and positive energy equilibrium (Chen et al. 2015; Borgmann et al. 2021; Beutler et al. 2017; Su et al. 2017; Alhadeff et al. 2019; Berrios et al. 2021). One potent inhibitor of $ARC^{AgRP/NPY+}$ neurons is the anorexigenic hormone leptin, which directly hyperpolarizes and silences $ARC^{AgRP/NPY+}$ neurons during states of energy surplus (Takahashi and Cone 2005; Baver et al. 2014; Bermeo et al. 2020). To ascertain the responses of ARC^{Drd1+} neurons to leptin, we performed whole cell patch clamp electrophysiology on ARC^{Drd1+} and $ARC^{AgRP/NPY+}$ neurons and measured changes in firing rate and membrane potential after a 3 minute of perfusion of 100 nM leptin (Figure 2). As expected, bath application of leptin decreased the firing rate of all $ARC^{AgRP/NPY+}$ neurons from control and fasted animals (Figures 2A-C). Additionally, leptin significantly hyperpolarized all tested control and fasted $ARC^{AgRP/NPY+}$ neurons (Figure 2D). While leptin perfusion also inhibited the majority of ARC^{Drd1+} neurons, the hormone's effects were of smaller magnitude compared to responses observed in $ARC^{AgRP/NPY+}$ neurons. In control ARC^{Drd1+} neurons, bath application of leptin decreased firing rate of all tested neurons (Figures 2E-G). However, this reduction was only 64% on average, compared to an average 93% reduction in firing rate for control $ARC^{AgRP/NPY+}$ neurons, a difference that was not statistically significant (unpaired two-tailed Student's t-test, $p = 0.13$, $t = 1.64$, $df = 10$, $n = 6$ neurons per group). Additionally, while leptin perfusion significantly hyperpolarized control ARC^{Drd1+} neurons, only 83% of tested neurons had a reduction in membrane potential. Taken with our previous finding that ARC^{Drd1+} neurons had

insignificant changes in firing rates due to fasting (Figure 1C), these results indicate heterogeneity in terms of how ARC^{Drd1+} neurons respond to energy balance signals.

Figure 3: ARC^{Drd1+} neurons functionally connect other ARC neurons

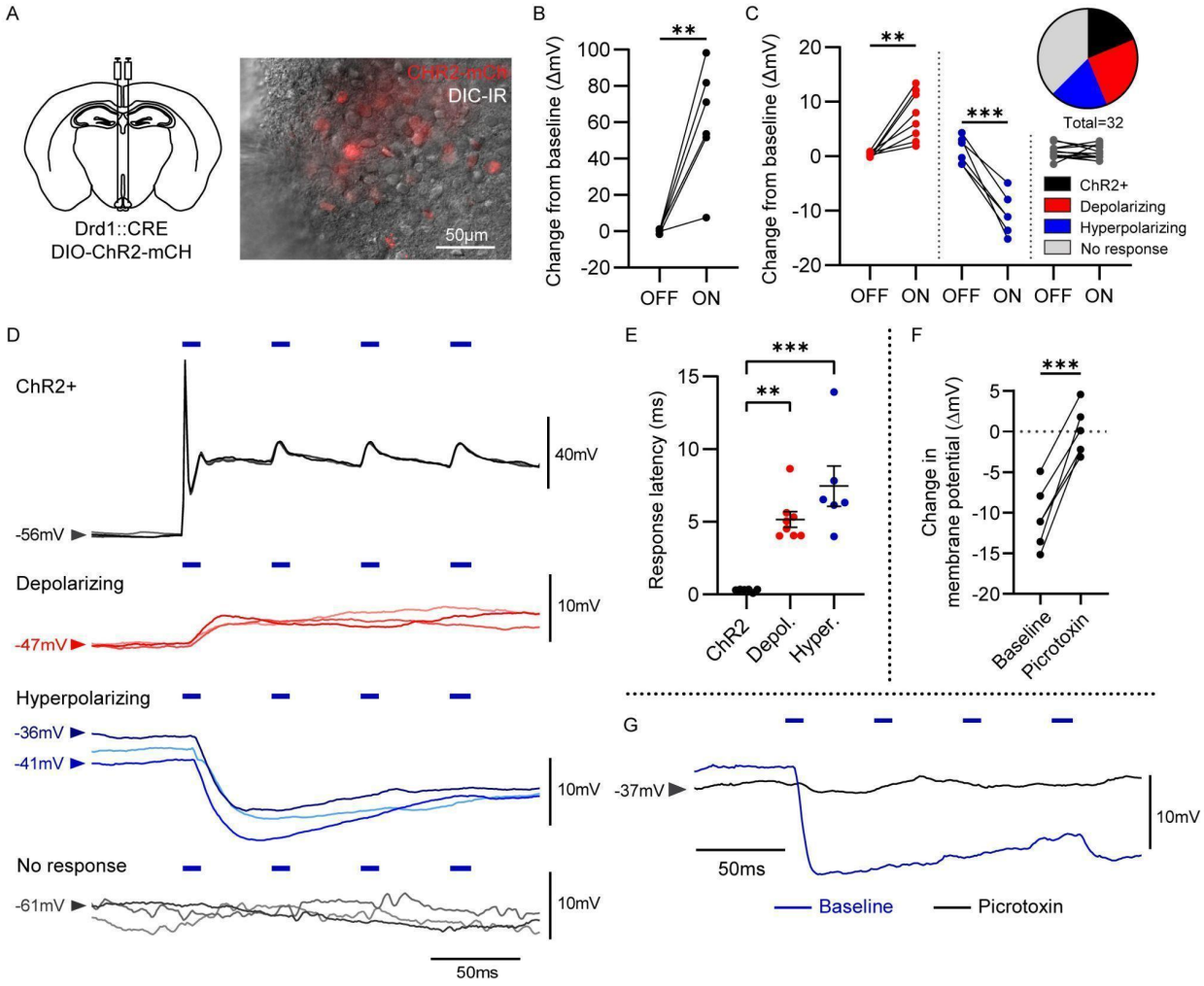

Figure 3 legend

A. Left: Schematic of bilateral intracranial injection of Cre dependent ChR2-mCh to the ARC of Drd1-Cre mice. Right: representative image of 40x DIC IR and fluorescence of ChR2-mCh ARC viral expression in acute coronal brain slices. Scale bar 50 μm.

B. Change in membrane potential for light off and on for ChR2 expressing neurons, (*p < 0.05, **p < 0.01, ***p < 0.001 as determined by paired two tailed Student's t-test, t = 4.763, df = 5, n = 6 pairs).

C. Change in membrane potential of ARC neurons which depolarized, hyperpolarized, or had no response to ARC^{Drd1+} ChR2 inputs. (*p < 0.05, **p < 0.01, ***p < 0.001 as determined by paired two tailed Student's t-test; depolarized: t = 4.763, df = 5, n = 8 pairs; hyperpolarized: t = 3.81, df = 5, n = 6 pairs); no response: t = 3.81, df = 5, n = 12 pairs). Top right: pie chart summary recorded responses in ARC neurons. (*p < 0.05, **p < 0.01, ***p < 0.001 as determined by paired two tailed Student's t-test).

D. Representative whole cell current clamp traces for responses to four light stimulations, three individual traces from the same neuron shown per response type.

E. Latency from light onset to response initiation for responding neurons. (*p < 0.05, **p < 0.01, ***p < 0.001 as determined by ordinary one-way ANOVA with Bonferroni post-hoc comparison, n = 6–8/group; F_{group} = 1.85 (2, 17), p = <0.001).

F. Change in membrane potential for hyperpolarizing neurons during baseline and after 5 minutes from the start of the perfusion of PTX. (*p < 0.05, **p < 0.01, ***p < 0.001 as determined by paired two-tailed Student's t-test, t = 8.440, df = 5, n = 6 pairs, p = <0.001).

G. Representative trace of extinction of hyperpolarization response after 5 minutes of PTX perfusion.

ARC^{Drd1+} neurons functionally connect to other ARC neurons

After comparing the effects of fasting and leptin on ARC^{Drd1+} neurons, we evaluated if other ARC neurons receive inputs from ARC^{Drd1+} neurons in the region. To achieve this, we injected an AAV carrying Cre dependent Channelrhodopsin-mCherry (ChR2-mCh) (Boyden et al. 2005) into the ARC of $Drd1^{cre/+}$ mice. We then performed patch clamp electrophysiology on randomly selected neurons in the ARC (Figure 3). This strategy allowed us to use Channelrhodopsin assisted circuit mapping (CRACM) (Petreanu et al. 2007; Atasoy et al. 2008) to interrogate the postsynaptic responses of ARC neurons following ARC^{Drd1+} neuron activation (Figures 3A-E).

We obtained current clamp recordings from 32 neurons in 19 coronal hypothalamic slices from 12 animals. Of these 32 neurons, we identified 6 neurons that expressed ChR2 (ChR2+), 8 neurons with postsynaptic depolarizations, 6 neurons with postsynaptic hyperpolarizations, 12 neurons with no discernible response (Figures 3B and 3C). Light stimulation in ChR2+ neurons resulted in a significant change in peak membrane potential from baseline (Figure 3B) and the latency of the response for these neurons was 0.30 ± 0.04 ms (Figure 3E), consistent with the temporal kinetics of ChR2-based neuron activation (Boyden et al. 2005). Light stimulation did not result in a significant change in peak membrane potential from baseline in non-responders but was significant for neurons with depolarizing and hyperpolarizing responses (Figure 3C). Latency of the response from onset of the light stimulus for depolarizing and hyperpolarizing neurons was 5.16 ± 0.54 ms and 7.46 ± 1.39 ms, respectively (Figure 3E). Because these neurons often demonstrate spontaneous firing and occasionally show postsynaptic depolarization

resulting in action potentials, only traces where the analysis window was free of action potentials were analyzed, likely resulting in underestimation of the strength of depolarizing inputs to these neurons. One hyperpolarizing neuron was observed to have an average response latency of 13.9 ms, suggesting the input may have originated from a neuron with an intermediary connection to an upstream ChR2 expressing neuron. Bath perfusion of ACSF containing 100 μM of the gamma aminobutyric acid (GABA) receptor blocker picrotoxin (PTX) resulted in a significant reduction in the hyperpolarizing response in all tested neurons (Figures 3F and 3G). On average, response magnitudes decreased by 10.46 ± 1.23 mV, confirming the hyperpolarizing inputs observed were GABAergic.

Figure 4: ARC^{Drd1+} neurons make functional connections to ARC$^{AgRP/NPY+}$ neurons, and ARC$^{AgRP/NPY+}$ neurons include a subpopulation of ARC^{Drd1+} neurons

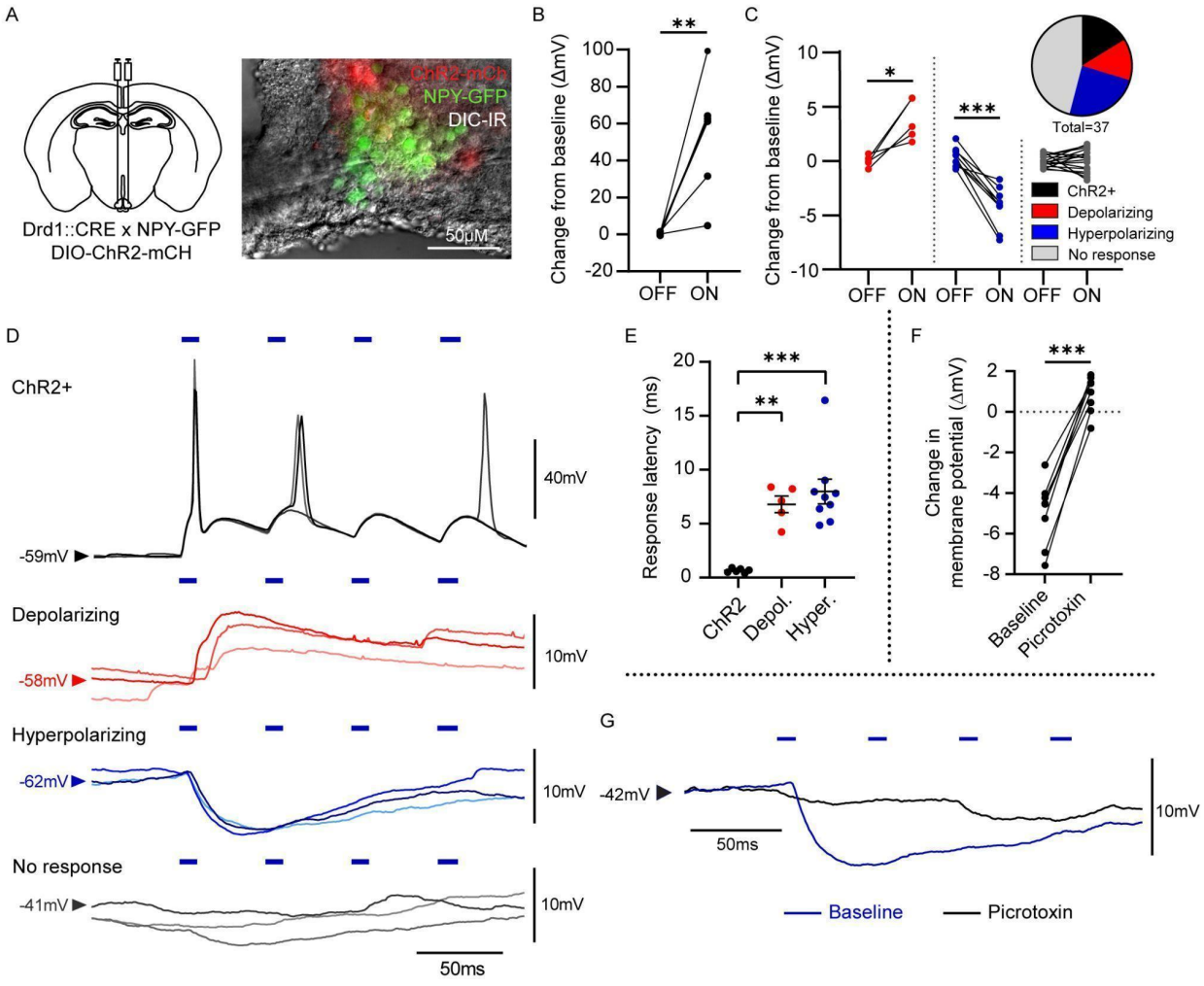

Figure 4 Legend

A. Left: schematic of bilateral intracranial injection of Cre dependent ChR2-mCherry (ChR2-mCh) to the ARC of Drd1$^{Cre/+}$;NPY$^{Gfp/+}$ mice. Right: representative image

of 40x DIC IR and fluorescence of ChR2-mCh ARC viral expression and ARC NPY-GFP expression in acute coronal brain slices. Scale bar 50 μm.

B. Change in membrane potential for light off and on for ChR2 expressing $ARC^{AgRP/NPY+}$ expressing neurons (*p < 0.05, **p < 0.01, ***p < 0.001 as determined by paired two tailed Student's t-test, t = 4.038, df = 5, n = 6 pairs). Analysis was conducted in an identical manner to those in Figure 3B.

C. Change in membrane potential of $ARC^{AgRP/NPY+}$ neurons that depolarized, hyperpolarized, or had no response to ARC^{Drd1+} ChR2 inputs. (*p < 0.05, **p < 0.01, ***p < 0.001 as determined by paired two tailed Student's t-test; depolarized: t = 4.149, df=4, n = 5 pairs; hyperpolarized: t = 7.494, d f= 8, n = 9 pairs); No response: t = 0.1774, d f= 16, p = 0.861, n = 12 pairs). Top right: pie chart summary for responses recorded in $ARC^{AgRP/NPY+}$ neurons (*p < 0.05, **p < 0.01, ***p < 0.001 as determined by paired two tailed Student's t-test, t = 4.149, df=4, n = 5 pairs). Analysis was conducted in an identical manner to those in Figure 3C.

D. Representative whole cell current clamp traces for various responses to light stimulation, three individual traces from the same $ARC^{AgRP/NPY+}$ neuron shown per response type.

E. Latency from light onset to response initiation for responding $ARC^{AgRP/NPY+}$ neurons. (*p < 0.05, **p < 0.01, ***p < 0.001 as determined by ordinary one-way ANOVA with Bonferroni post-hoc comparison, n = 5–9/group; F_{group} = 1.61 (2, 17), p = <0.001. Analysis was conducted in an identical manner to those in Figure 3E.

F. Change in membrane potential for hyperpolarizing $ARC^{AgRP/NPY+}$ neurons during baseline and after 5 minutes from the start of PTX perfusion. (*p < 0.05, **p < 0.01, ***p < 0.001 as determined by paired two-tailed Student's t-test, t = 14.2, df = 7, n = 8 pairs, p = <0.001). Analysis was conducted in an identical manner to those in Figure 3F.

G. Representative trace of extinguishment of hyperpolarization response of $ARC^{AgRP/NPY+}$ neurons during baseline and after 5 minutes of PTX perfusion.

ARC^{Drd1+} neurons possess functional connections to $ARC^{AgRP/NPY+}$ neurons, and $ARC^{AgRP/NPY+}$ neurons include a subpopulation of ARC^{Drd1+} neurons

Given their anatomical location, $ARC^{AgRP/NPY+}$ neurons likely comprised a substantial subgroup of neurons we recorded from during our initial CRACM experiment (Figure 3). Thus, we hypothesized that some ARC^{Drd1+} neurons may have functional inputs to $ARC^{AgRP/NPY+}$ neurons. To investigate this connection, we injected an AAV carrying Cre-dependent ChR2-mCherry into the ARC of $Drd1^{cre/+}$;$NPY^{Gfp/+}$ mice resulting in green labeled $ARC^{AgRP/NPY+}$ cells and red labeled ARC^{Drd1+} cells. We then performed patch clamp electrophysiology on GFP labeled $ARC^{AgRP/NPY+}$ neurons, allowing us to evaluate the presence of functional inputs (Figure 4).

We obtained current clamp recordings from 37 $ARC^{AgRP/NPY+}$ neurons in 13 coronal hypothalamic slices from 9 mice. Of these ARC^{NPY+} neurons, we identified 6 ChR2+ neurons, 5 neurons with postsynaptic depolarizations, 9 neurons with postsynaptic hyperpolarizations, and 17 neurons with no discernible response (Figures 4B-D). ChR2

expression in $ARC^{AgRP/NPY+}$ neurons confirms that a subpopulation of ARC^{Drd1+} neurons are also AgRP/NPY positive, in line with previous findings (Zhang and van den Pol 2016). Light stimulation in ChR2+ $ARC^{AgRP/NPY+}$ neurons resulted in a significant change in peak membrane potential from baseline (Figure 4B), and the latency of the response for these neurons was 0.65 ± 0.08 ms (Figure 4E). For $ARC^{AgRP/NPY+}$ neurons which were classified as non-responding, light stimulation did not result in a significant change in peak membrane potential compared to baseline but was significant for both depolarizing and hyperpolarizing $ARC^{AgRP/NPY+}$ neurons (Figure 4C). Latency of the response from onset of the light stimulus for depolarizing and hyperpolarizing $ARC^{AgRP/NPY+}$ neurons was 6.80 ± 0.77 ms and 7.98 ± 1.15 ms, respectively (Figure 4E). One hyperpolarizing $ARC^{AgRP/NPY+}$ neuron was observed to have an average response latency of 16.42 ms, again suggesting the input may have originated from a neuron with an intermediary connection to an upstream ChR2 expressing neuron. Bath perfusion of ACSF containing 100 μM PTX resulted in a significant reduction in the hyperpolarizing response in all tested $ARC^{AgRP/NPY+}$ neurons (Figures 4F and 4G). On average, response magnitudes decreased by 5.84 ± 0.41 mV, confirming that the hyperpolarizing inputs from ARC^{Drd1+} neurons → $ARC^{AgRP/NPY+}$ neurons observed were GABAergic.

Discussion

Responses of ARC^{Drd1+} neurons to signals of metabolic deficit and surplus

We show leptin inhibits ARC^{Drd1+} neurons in a comparable manner to responses observed in the ARC$^{AgRP/NPY+}$ neuronal population. Other patch clamp studies have focused on the effects of small molecules on ARC neurons including leptin (Glaum et al. 1996; Cowley et al. 2001; van den Top et al. 2004; Vong et al. 2011; Takahashi and Cone 2005; Hill et al. 2008), ghrelin (Tong et al. 2008; Kohno and Yada 2012), DA and DA receptor agonists and antagonists (Zhang and van den Pol 2016; Alhadeff et al. 2019), insulin (Mirshamsi et al. 2004; Kohno and Yada 2012), and glucose (Kohno and Yada 2012; Jais et al. 2020). Our results regarding leptin's action on ARC$^{AgRP/NPY+}$ neurons are in line with previous studies demonstrating leptin-based inhibition of this neuron subtype (Takahashi and Cone 2005; Baver et al. 2014). Similar responses observed in ARC^{Drd1+} neurons may be explained partially by incidental targeting of the ARC$^{Drd1+;AgRP/NPY+}$ neuron population, which was identified during subsequent CRACM experiments. Interestingly, profiling of the spontaneous firing and membrane properties of ARC^{Drd1+} neurons revealed that, as a whole, they are less responsive than ARC$^{AgRP/NPY+}$ neurons to fasting. Others have also measured the electrophysiological properties of ARC neurons given different experimental treatments, including fasting (Liu et al. 2012), exercise (Han et al. 2018), high fat diet (HFD) (Baver et al. 2014; Wei et al. 2015; Jais et al. 2020), and gastric inputs (Alhadeff et al. 2019; Goldstein et al. 2021; Jais et al. 2020). Ultimately, our results suggest the ARC^{Drd1+} neuronal population is heterogeneous.

Connectivity of ARC^{Drd1+} and $ARC^{AgRP/NPY+}$ neurons

Our CRACM experiments revealed overlap of ARC^{Drd1+} neurons with $ARC^{AgRP/NPY+}$ neurons, presenting a potential site of direct regulation by dopaminergic inputs from the midbrain or other regions. Interestingly, we identified two subpopulations of ARC^{Drd1+} neurons which had either GABAergic or depolarizing outputs to $ARC^{AgRP/NPY+}$ neurons. We consider it unlikely that ARC^{Drd1+}→$ARC^{AgRP/NPY+}$ neuron connections were in fact AgRP→AgRP or POMC→AgRP connections, given previous findings on the connectivity of ARC neurons. Studies identified functional AgRP→POMC connections, but failed to find functional interconnections within AgRP and POMC populations (i.e., AgRP→AgRP and POMC→POMC) (Atasoy et al. 2012). Additionally, no evidence of POMC→AgRP connectivity has been identified, despite early speculation of feedback loops (Betley et al. 2013). Thus, ARC^{Drd1+}→$ARC^{AgRP/NPY+}$ neurons (i.e. ARC^{Drd1+} neurons which putatively do not express AgRP/NPY) represent a unique group of neurons with differential inputs to $ARC^{AgRP/NPY+}$ neurons.

DA signaling in the ARC

Our findings instantiate both direct and indirect mechanisms through which ARC^{Drd1+} neuronal populations could modulate the $ARC^{AgRP/NPY+}$ circuit. Our CRACM experiments confirm the existence of an $ARC^{Drd1+;AgRP/NPY+}$ neuronal population, supporting previous findings that Drd1-dependent signaling can drive direct activation of $ARC^{AgRP/NPY+}$ neurons (Zhang & van den Pol, 2016). Synapses containing DA have been localized to the soma of $ARC^{AgRP/NPY+}$ neurons (Zhang & van den Pol, 2016), however the circumstances that precipitate DA release at these terminals are unknown. Our lab

recently found that mice fed a HFD have increased DA tone in other hypothalamic regions containing Drd1 expressing neurons (Grippo et al., 2020), and the occurrence of a comparable phenomenon in the ARC remains a distinct possibility. In one proposed model, palatable food would drive increased DA input to $ARC^{Drd1+;AgRP/NPY+}$ neurons, which in turn become activated by Drd1 Gα/s-type G-coupled protein receptor signaling. This might be complemented by parallel DA release to POMC neurons, which are directly inhibited by Ga/i coupled dopamine receptor 2 (Drd2) signaling (Zhang & van den Pol, 2016). Such signaling could drive increased feeding, perhaps even in sated animals, but the specific molecular pathways underlying DA receptor signaling in ARC neuron subtypes is unknown.

In addition to the $ARC^{Drd1+;AgRP/NPY+}$ neuronal population, we identified two additional groups of ARC^{Drd1+} neurons which had inhibitory or excitatory inputs to $ARC^{AgRP/NPY+}$ neurons. The circumstances driving activation of various ARC^{Drd1+} subtypes are unknown, and different signals may elicit distinct $ARC^{Drd1+}\rightarrow ARC^{AgRP/NPY+}$ inputs. However, evidence supports DAergic mediated inhibition of $ARC^{AgRP/NPY+}$ neurons in response to gastric signals. In experiments performed by Alhadeff *et al.*, intragastric infusions of nutrients and ethanol increased midbrain DA signaling and inhibited $ARC^{AgRP/NPY+}$ neurons. Infusion of a DA receptor antagonist cocktail was shown to dampen these inhibitory responses during reward delivery (Alhadeff et al. 2019), but the direct inputs and mechanism underlying this DA signaling was not elucidated. The findings are notably counterintuitive to the results presented by Zhang *et al.*, who observed that DA and the Drd1 selective agonist SKF 38393 excite AgRP neurons (Zhang & van den Pol, 2016). Our work provides a bridge between these results, showing ARC^{Drd1+} neurons can both

activate or inhibit $ARC^{AgRP/NPY+}$ neurons. This supported by the growing body of evidence that DA and Drd1 can have differential actions in the same brain region (Trudeau et al. 2014; Miller et al. 2019), supporting this Miller *et al.* showed different medial amygdala dopamine 1 receptor (MeApv-D1R) neurons can possess outputs with divergent functional connections, where MeApv-D1R neurons send excitatory outputs to the dorsal medial region of the ventromedial hypothalamus (VMHdm) and inhibitory projections to the bed nucleus of the stria terminalis (BNST) (Miller et al. 2019). Further highlighting the potential complexity of the system, Miller *et al.* found that the selective Drd1 agonist SKF 81297 increased the excitability of BNST projecting MeApv-D1R neurons, while decreasing the excitability of VMH projecting MeApv-D1R neurons. Only with retrograde labeling of MeApv-D1R projections were the investigators ultimately able to distinguish these two subpopulations of $Drd1^{cre/+}$-$tdTomato^{td/+}$ labeled neurons in the same nucleus. An analogous phenomenon may be occurring in populations of ARC^{Drd1+} neurons in our study. ARC^{Drd1+} neurons in close proximity may possess differential responses to the same factor, and complete functional characterization of distinct ARC^{Drd1+} subpopulations will require segmentation by inputs, projections, and additional markers.

Limitations of the Study

Leptin signaling can have differential effects in different subgroups of ARC neurons. Because this study focused on leptin's inhibitory actions, we cannot rule out the possibility that some ARC^{Drd1+} neurons would have had responses to leptin that are not typically detectable in quiescent or hyperpolarized neurons with membrane potentials below -50mV (Smith et al. 2018). Furthermore, this report describes the electrophysiological

properties and functional connections of a specific subset of neurons labeled by Drd1-Cre and NPY-GFP, and while these transgenic systems have been previously used to corroborate the presence of functional Drd1 and Npy protein or mRNA in labeled neurons (Heusner et al. 2008; van den Pol et al. 2009; Zhang and van den Pol 2016; Miller et al. 2019), this study did not validate functional signaling in the ARC neurons of these mice. Future studies will evaluate the response of ARC^{Drd1+} neurons to DA and selective agonists to further examine the role ARC Drd1 signaling plays in shaping animal behavior and metabolism.

Methods

RESOURCE AVAILABILITY

Lead contact and Materials availability

This study did not generate new unique reagents or mouse lines. Further information and requests should be directed to and will be fulfilled by the Lead Contact, Ali D. Güler (aguler@virginia.edu).

EXPERIMENTAL MODEL AND SUBJECT DETAILS

All animal experiments were conducted in compliance with the University of Virginia Institutional Animal Care and Use Committee (IACUC). Animals were provided cotton nesting material (Ancare, Bellmore, NY) and animal cages were individually ventilated and temperature and humidity controlled, (approx. 40% humidity, 22°C–24°C). Animals were housed on a 12-hour light/dark cycle, and given water and food ad libitum, except

for approved periods of time during fasting experiments. The following mouse lines were used: Drd1$^{tm1(cre)Rpa}$ (Heusner et al. 2008), Gt(ROSA)26Sor$^{tm14(CAG-tdTomato)Hze}$, (Madisen et al. 2010), Tg(Npy-hrGFP)1Lowl (van den Pol et al. 2009). Drd1$^{(Cre/Cre)}$ (KO) mice and littermates bred for husbandry were raised on standard chow diet PicoLab Rodent Diet 20 5053 (LabDiet, USA) placed on the cage floor to facilitate access to the food for the Drd1-KO mice.

METHOD DETAILS

Mouse diets

Standard chow diet (SCD): PicoLab Rodent Diet 20 5053 (3.07 kcal/gram; 13% fat, 24% protein, 62% carbohydrates; 3.2% sucrose).

Viral Expression and Stereotaxic Surgery

All surgery was performed on mice between 8 and 14 weeks of age using aseptic technique in compliance with the University of Virginia IACUC. Surgical anesthesia was induced with 5% isoflurane (Isothesia) and then maintained at 2% to 2.5% throughout the procedure. After induction animals were mounted in a stereotaxic frame (Kopf) with an electric heating pad underneath to maintain body temperature. Veterinary ocular lubricant was used on each animal's eyes and reapplied as necessary to prevent dehydration/desiccation. A recombinant AAV was used to express a specific transgene, containing a double-floxed inverted open reading frame (DIO cassette). Virus was delivered at 100nl/min by a microsyringe pump controller (World Precision Instruments, model Micro 4), via a 10 µL syringe (Hamilton) and 26-gauge needle (Hamilton). After

infusion of the AAV was completed, the syringe was left in place for 10 min, after which it was retracted 0.2mm and then left in place for another 10 minutes before being withdrawn completely. As an analgesic, for 24 hours before and for three days after surgery mice were provided with 30 mg/kg ibuprofen drinking solution (4.7 ml Children's Motrin dissolved in 500 ml sterile water). Mice were then sacrificed for optogenetic experiments 6 to 11 weeks after intracranial injections.

Viral constructs

AAV1-hSyn-ChR2(H134R)-mCherry (300nl; diluted to ~1.2x10^12 viral genomes/ul with sterile PBS) was injected into the ARC (ML: ± 0.29 mm, AP: - 0.30 mm, DV: −5.75 mm). All coordinates are relative to bregma (George Paxinos and Keith B. J. Franklin).

Slice electrophysiology

Acute brain slice preparation methods including Na+ spike protocol were adapted from (Ting et al. 2014; Ting et al. 2018). When preparing acute brain slices from surgery animals, mice were IP injected with a mixture of ketamine/xylazine and transcardially perfused with roughly 30ml of ice cold NMDG-ACSF containing in mM: 93 NMDG; 2.5 KCl, 1.2 NaH2PO4, 30 NaHCO3, 20 HEPES, and 25 dextrose, 5 sodium ascorbate, 2 thiourea, 3 sodium pyruvate, 10 MgSO4.7H2O, 0.5 CaCl2.2H2O, saturated with 95% O2 and 5% CO2. The brain was then rapidly dissected and 300uM sections containing the hypothalamus were taken using a Compresstome VF-200 in ice cold NMDG-ACSF. Slices were incubated in 34°C NMDG-ACSF and after completion of the Na+ spike protocol (Ting et al. 2018) the slices were transferred to a high HEPES low Ca2+ buffer holding buffer at 34°C and allowed to come to room temperature where they were held

until transfer to microscope for recording. HEPES buffer contained in mM: 92 NaCl, 2.5 KCl, 1.2 NaH2PO4, 30 NaHCO3, 20 HEPES, and 25 dextrose, 5 sodium ascorbate, 2 thiourea, 3 sodium pyruvate, 10 MgSO4.7H2O, 0.5 CaCl2.2H2O, saturated with 95% O2 and 5% CO2. Mice lacking ChR2 expression or which had mistargeting of the viral infusion, were not included in this study. For non-surgery animals, mice ages P31 to P58 were decapitated after being deeply anesthetized with isoflurane using the jar drop method. Brains were rapidly dissected and mounted for slicing in the compresstome slicer. Slices were taken ice cold sucrose cutting solution containing (in mM): 200 sucrose, 26 NaHCO3, 1.25 Na2HPO4, 3.5 KCl, 10 glucose, 3.8 MgCl2, 1.2 MgSO4, pH was adjusted to 7.3 to 7.4 and osmolarity ranged from 299 to 302 mOsm (Whitt and Meredith 2016). Slices were then transferred to the same high HEPES low Ca2+ holding buffer described above at 34°C and allowed to come to room temperature where they were held until transfer to microscope for recording. In all experiments slices were allowed to rest for a minimum of 45 minutes before transfer to a Slicescope 6000 microscope with 4x dry and 40x water immersion Nikon objectives. For all whole cell current clamp recordings, the bath was superfused with a continuous flow (2.5 ml/min) of recording aCSF at room temperature (26°C to 28°C), containing the following (in mM): 119 NaCl, 2.5 KCl, 1.25 NaH2PO4, 24 NaHCO3, 12.5 glucose, 2 mM CaCl2·4H2O and 2 mM MgSO4·7H2O, saturated with 95% O2 and 5% CO2 (Ting et al. 2018). For all extracellular solutions, osmolarity ranged from 299 to 302 mOsm and pH was adjusted with strong HCl and ranged from 7.3 to 7.4. Coronal slices containing the ARC were identified visually by the shape of the both 3rd ventricle and the presence of medial eminence. To target $ARC^{AgRP/NPY+}$ neurons for patching, NPY-GFP fluorescence was excited and visualized

using a pE-300-white LED light source and GFP filter set. Images of patched brain regions were taken using Scientifica camera and Ocular imaging software. A Multiclamp 700B amplifier and Digidata 1550B digitizer (Molecular Devices) were used to perform all patch clamp experiments. Voltage measurements were digitized at 50 kHz and bridge balance was monitored closely. All experiments were conducted using 3-6MΩ microelectrodes pulled with a Sutter P97 puller. For all current clamp recordings, the pipette was backfilled with an intracellular solution adapted from (Miller et al. 2019) containing, in mM: 135 K-gluconate, 10 HEPES, 3.5 NaCl, 1 EGTA, 5 Mg-ATP, 0.5 Na3-GTP. For intracellular solution, osmolarity ranged from 290 to 295 and pH was adjusted with KOH and ranged from 7.3 to 7.4. For each neuron, recordings measuring spontaneous firing rate were taken each lasting a minimum of 90 seconds. No holding current was used during whole cell recordings of spontaneous firing. Offline the recordings were analyzed using a combination of ClampFit (Molecular devices) and custom scripts in Matlab (Mathworks) software. Statistical tests were performed in Prism 9 (Graphpad). Light stimulation consisted of 10ms square pulses of light delivered at 20Hz (10 pulses total). Light stimulation was delivered by the high (40x) magnification objective to a hexagonal area approximately 250 μM diameter centered on the recorded cell, and the same light intensity maintained all recordings. To report changes in membrane potential and latency in CRACM experiments, 3 to 6 traces (typically 5 or 6 traces) were analyzed. Non-responding cells were confirmed to be healthy by either observation of normal spontaneous firing or minor current injection to elicit action potentials. For each trace the absolute peak value reached relative to baseline was identified within the 50ms immediately after stimulus onset. Results were then averaged for all traces analyzed for

that recording. Some neurons spontaneously fired action potentials during the pre or post stimulus analysis window, and traces where this occurred were excluded from analysis, and only cases where the analysis window fell within an inter spike interval were included. For all experiments involving drug perfusions, recordings were acquired only in slices previously treated with pure ACSF. After drug perfusion and washout, no more recordings were made and that slice was discarded. Firing threshold was calculated using scripts adapted from code made available by Mathieu Noe on the Mathworks website (Noe 2021).

Quantification and Statistical Analysis

When comparing two groups of normally distributed data, a Student's two tailed t test was used. To compare the effects of genotype and fasting within 4 groups, two-way ANOVA test was used. When data was collected from the same animals across time, a three-way ANOVA test was performed to analyze time, genotype and fasting effect. In experiments with a single variable and more than two groups, a one-way ANOVA was performed. Following a significant effect in the ANOVA test, Bonferroni's post hoc comparison was used to determine differences between individual data points. Analyses were conducted using the GraphPad Prism 9 statistical software for Windows. All data are presented as means ± standard error of the mean with $p < 0.05$ considered statistically significant.

Acknowledgments

We are especially thankful for technical assistance from Qi Zhang, Qijun Tang, Ryan Grippo, Aundrea Rainwater, and Tarun Vippa. We are also grateful to Ignacio Provencio, Masashi Kawasaki, Manoj Patel, and Christopher Deppmann for their feedback.

This work was supported by NIH National Institute of General Medicinal Sciences R01GM121937, 1R35GM140854 (A.D.G.), UVA Brain Institute 2018 Seed Funding Award (A.D.G.).

Author contributions

S.R.C. conceived, designed, and performed all experiments, with input from A.D.G.. S.R.C. wrote the manuscript with input from A.D.G.

Declaration of interests

The authors declare no competing interests.

Chapter 4: Outlook

Summary

Today, a primary objective of neuroscience is to generate a complete connectome of mammalian nervous systems. In the last few decades, advances in technology and techniques have driven major discoveries of the electrophysiological properties, connectivity, and molecular mechanisms of individual neurons. However, many obstacles exist in the path to a complete elucidation of the molecular mechanisms and circuits which underpin animal behavior and consciousness, including their relevance to the betterment and enhancement of the human condition. The rise of cell type specific transgenic systems, aided by CRISPR/Cas9 and other gene editing tools, has identified different neuronal populations in the hypothalamus and brain that have essential homeostatic functions. In this dissertation, I contribute to this ongoing work by characterizing Drd1 expressing neurons in the SCN and ARC, including their functional connectivity and the impacts of DA signaling in these regions. However, our understanding of DA's role in modulating food intake and circadian rhythms remains incomplete. The hypothalamus is exceptionally heterogeneous, and ongoing efforts to fully characterize hypothalamic circuits face major challenges. Additionally, the limitations of widely used tools, such as genetically encoded actuators or cell type specific markers, are non-trivial and increasingly relevant. First, this chapter discusses the challenges of interrogating heterogeneous populations of neurons. Second, we examine difficulties inherent to

studying the effects of metabotropic signaling on neuron membrane properties. Third, we describe best management practices when using genetically encoded actuators and performing hypothalamic patch clamp electrophysiology. Finally, we discuss future work and challenges in understanding DA in the brain.

The heterogeneity of hypothalamic neuronal populations complicates scientific efforts to characterize them

Cell type specific markers are molecular hallmarks which enable scientists to target specific populations of neurons during experiments, such as transcripts, cell surface proteins, or internal factors. In transgenic systems, alleles or regulatory elements can be modified to confer specificity for a given cell marker, allowing experimenters to selectively label and manipulate cells which share some homology in protein expression or gene regulation. Cell specific marking and transgenic systems have proved invaluable tools for linking neuronal activity with animal behavior. For instance, in ARC research, cell type specific activation of AgRP neurons with genetically encoded actuators was instrumental in elucidating homeostatic circuits of food intake and orexigenic behavior (Aponte et al. 2011; Krashes et al. 2011; Atasoy et al. 2012; Betley et al. 2013). These tools have also allowed scientists to perform cell lineage tracing, leading to significant advances in our understanding of neural development. Use of cell markers has become ubiquitous, but we are now faced with the realization that the value of a given label is only as good as its specificity. Single cell transcriptomics has revealed heterogeneity within previously

grouped cell types in the hypothalamus and other brain regions (Campbell et al., 2017), and cell type specific labeling can mark neurons in the same nucleus or brain region that possess completely different functions or gene expression profiles. For instance, transgenic labeling of Slc6a1, the gene which encodes the mouse sodium- and chloride-dependent GABA transporter 1 (Slc6a1), broadly labels GABAergic neurons throughout the body and nervous system. While inherently useful for detecting GABAergic neurons in a given region, many unique cell types can be co-labeled by this Slc6a1, even in the same nucleus. Failure to account for the possibility of over-labeling can lead to overly broad conclusions about the function of neurons in close proximity. In these cases, multiple neuronal subpopulations may be targeted for expression of genetically encoded tools or selected for recording during patch clamp experiments. Thus, experimenters must take additional steps to improve the specificity of experiments and to reach deeper conclusions. Several strategies have been utilized to enhance the specificity of cell marker experiments. Using one or more additional cell markers to perform intersectional studies within a given group of neurons is one such strategy (Fenno et al., 2014) but requires breeding dual or triple transgenic animals which lowers experimental throughput due to the increased time and resources often required to breed and genotype such animals. Another strategy is *post hoc* verification of other aspects of a given cell, such as use of biocytin labeling of patched neurons, which can reveal morphological and immunological differences between similarly labeled cells in the same experiment. Ultimately, more tools and strategies will be needed to describe state specific differences or subgroups in neuronal populations.

Characterizing the effects of metabotropic receptor signaling on neuron membrane properties remains challenging

A central goal in connectivity research is to attain complete descriptions of the inputs to a given neuron or neuronal population. Ionotropic signaling, mediated by neurotransmitters which regulate ion channels, has been the major focus of patch clamp experiments characterizing neuron to neuron communication. This is unsurprising, given that voltage and current clamp techniques are well suited for detection of ion channel activity and changes in membrane conductances. Lesser studied are the mechanisms underlying changes in neuron excitability which occur as a consequence of metabotropic signaling. This is probably because such signaling events, including those mediated by GPCRs and other intracellular signaling, often have effects which occur on timescales greater than minutes. Metabotropic signaling can have profound effects on neuron membrane properties which last hours or days, ranging from changes in intrinsic excitability and conductances to remodeling of axonal and dendritic processes. Additionally, these effects can be indirect and change as the signaling cascades progress. This is reflected in early experiments characterizing Drd1-dependent signaling in medium spiny neurons (MSNs), where selective Drd1 agonists were not observed to cause immediate changes in spontaneous electrical properties (i.e. agonists failed to elicit spontaneous firing or dramatic changes in membrane potential). In fact, Ga/s and Drd1 signaling can have profound effects on membrane properties of neurons, and injections

of depolarizing current in MSNs revealed Drd1 agonist mediated changes in intrinsic excitability. Compared to controls, Drd1 agonist-treated MSNs initially fired more action potentials in response to current injections, although this excitability decreased after ten minutes (Hernández-López et al., 1997). Technical aspects of the patch clamp technique compound the difficulty of acquiring reliable results in such experiments. Longer recordings are more likely to be affected by pipette seal instability, and the dialysis of intracellular compartments by intracellular solutions can distort signaling events in traditional whole cell experiments. Perforated patching, which does not dilute intracellular factors, has emerged as one of the most promising techniques for studying receptor mediated changes in neuron excitability (Lahiri & Bevan, 2020). However, this technique also suffers from low throughput, as the experimenter must wait for adequate pore formation and access before data acquisition can begin. Optical techniques, including calcium imaging and genetically encoded voltage sensors, have also shown promise, as these methods minimize disruption of intracellular signaling. However, these techniques involve estimation of voltage or current changes based on photic detections, limiting their ability to finely interrogate electrical events inside neurons. Additionally, these techniques require expression of a sensor protein and suffer from limited temporal resolution.

Practical considerations for experimenters using patch clamp electrophysiology and genetically encoded actuators

Activation of AgRP cells during behavioral experiments induce voracious feeding, but researchers should be mindful that in-vivo chemogenetic and optogenetic experiments are unlikely to faithfully replicate endogenous outputs of those cells in question. The magnitude and other properties of cell activation depend directly on how a given actuator protein is expressed and how it is activated during experiments. Thus, stimulation via a genetically encoded actuator such as ChR2 or HM3Dq may result in activation that is artificially strong or temporally incongruous with endogenous outputs (K. S. Smith et al., 2016). Ultimately, the experimenter is responsible for controlling, reporting, and interpreting experiments in an unequivocal manner, and should employ best management practices to this end. Several strategies to minimize unintended effects during actuator experiments have been described. For instance, after behavioral experiments some researchers have blindly verified ChR2 vs control AAV targeting and expression levels (Aponte et al., 2011; Atasoy et al., 2012). Additionally, several studies have utilized experimental paradigms which varied the frequency of stimulus delivery or the magnitude of irradiance in a graded manner, as an approach to identify the minimum strength and frequency of inputs that achieve a desired threshold of output or effect (Aponte et al., 2011; Atasoy et al., 2012; Banghart et al., 2004; Petreanu et al., 2007). CNO and clozapine, the drugs used to activate DREADDs, have both been shown to have off-target

effects, and should be used at the lowest dose possible to avoid accidental signaling by endogenous receptors (Manvich et al., 2018). Actuators notwithstanding, experimenters performing circadian electrophysiology should take care to standardize time of acute brain slice preparation across experiments and report relevant zeitgeber or circadian times where possible.

Future directions for Drd1 research

As discussed throughout this dissertation, the consequences of Drd1 activation are multifaceted and cell specific. Strategies for examining Drd1 function are numerous and can generally be broken into two categories: identifying protein expression and localization, and functional assays of signaling and membrane properties. To identify expression and localization of Drd1 mRNA and Drd1 protein, studies have used fluorescent in-situ hybridization and immunohistochemistry, radiolabeled ligand binding studies, and RNAseq. Functional assays for Drd1 expression and signaling are mainly based on pharmacological approaches using selective agonists and antagonists, and include in-vitro cell assays, calcium imaging, brain slice electrophysiology, c-Fos staining, *in vivo* fluid cannulation and behavioral tests. Researchers have generated several transgenic mouse models to study Drd1, which allow for a range of capabilities such as genetic targeting of Drd1a::cre neurons (Madisen et al., 2010), Drd1-tomato fusion protein animals (Shuen et al., 2008), and animals where Drd1a is flanked by Flox sites, which allow for Cre-mediated selective ablation of Drd1 (Sariñana et al., 2014). In tandem with these methods, researchers also use approaches to identify release of DA and identification of DAergic fibers including immunohistochemistry against DA, TH, and DAT,

fast scan cyclic voltametry, HPLC of DOPAC/DA turnover ratios, and most recently engineered fluorescent *in vivo* DA sensors which can detect DA or ligand binding (Patriarchi et al., 2018). While these techniques have provided invaluable insights into DA systems, challenges with these technologies remain. Antibody staining for membrane proteins can be challenging, and Drd1 is no exception. Additionally, Drd1 is expressed in neurons throughout development, and the longevity of Cre recombinase in Drd1a mRNA positive cells is unknown. Genetic techniques that rely on Cre induced reporters such as the Ai14 mouse may have TdTomato labeling in cells which only briefly expressed Cre from the Drd1a locus during development. Compounding this problem is the lack of knowledge of regulation of Drd1 membrane expression, as neurons with Drd1 mRNA expression may not have functional receptor signaling due to low membrane expression or receptor internalization. Finally, some techniques are insensitive to Ga/s signalling despite our knowledge that the receptor is activated. A good example of this can be found when looking at research conducted with Ga/s type DREADDs. A recent study found that activation of Ga/s DREADD in AgRP neurons of the arcuate nucleus was capable of inducing sustained increases in food intake (Nakajima et al., 2016). However, in contrast to the large depolarizing effects of the Gq DREADD, no acute changes in membrane potential or excitability were found for these cells despite the obvious behavioral phenotype. Regardless, these transgenic animals have been vital to studying Drd1, especially findings derived from experiments in knockout animals. Future work will better characterize these systems, and enhance our understanding of DA's role in behavior and disease.

References

Aalto, J., & Kiianmaa, K. (1984). Circadian rhythms of water and alcohol intake: effect of REM-sleep deprivation and lesion of the suprachiasmatic nucleus. *Alcohol* , *1*(5), 403–407.

Abe, K., Kroning, J., Greer, M. A., & Critchlow, V. (1979). Effects of destruction of the suprachiasmatic nuclei on the circadian rhythms in plasma corticosterone, body temperature, feeding and plasma thyrotropin. *Neuroendocrinology*, *29*(2), 119–131.

Abrahamson, E. E., & Moore, R. Y. (2001). Suprachiasmatic nucleus in the mouse: retinal innervation, intrinsic organization and efferent projections. *Brain Research*, *916*(1-2), 172–191.

Alhadeff, A. L., Goldstein, N., Park, O., Klima, M. L., Vargas, A., & Betley, J. N. (2019). Natural and Drug Rewards Engage Distinct Pathways that Converge on Coordinated Hypothalamic and Reward Circuits. *Neuron*, *103*(5), 891–908.e6.

Altherr, E., Rainwater, A., Kaviani, D., Tang, Q., & Güler, A. D. (2021). Long-term high fat diet consumption reversibly alters feeding behavior via a dopamine-associated mechanism in mice. *Behavioural Brain Research*, *414*, 113470.

Anand, B. K., & Brobeck, J. R. (1951). Hypothalamic control of food intake in rats and cats. *The Yale Journal of Biology and Medicine*, *24*(2), 123–140.

Andrews, Z. B., Liu, Z.-W., Walllingford, N., Erion, D. M., Borok, E., Friedman, J. M., Tschöp, M. H., Shanabrough, M., Cline, G., Shulman, G. I., Coppola, A., Gao, X.-B.,

Horvath, T. L., & Diano, S. (2008). UCP2 mediates ghrelin's action on NPY/AgRP neurons by lowering free radicals. *Nature*, *454*(7206), 846–851.

Aponte, Y., Atasoy, D., & Sternson, S. M. (2011). AGRP neurons are sufficient to orchestrate feeding behavior rapidly and without training. *Nature Neuroscience*, *14*(3), 351–355.

Atasoy, D., Aponte, Y., Su, H. H., & Sternson, S. M. (2008). A FLEX switch targets Channelrhodopsin-2 to multiple cell types for imaging and long-range circuit mapping. *The Journal of Neuroscience: The Official Journal of the Society for Neuroscience*, *28*(28), 7025–7030.

Atasoy, D., Betley, J. N., Su, H. H., & Sternson, S. M. (2012). Deconstruction of a neural circuit for hunger. *Nature*, *488*(7410), 172–177.

Atkinson, S. E., Maywood, E. S., Chesham, J. E., Wozny, C., Colwell, C. S., Hastings, M. H., & Williams, S. R. (2011). Cyclic AMP signaling control of action potential firing rate and molecular circadian pacemaking in the suprachiasmatic nucleus. *Journal of Biological Rhythms*, *26*(3), 210–220.

Baillie, P., & Morrison, S. D. (1963). The nature of the suppression of food intake by lateral hypothalamic lesions in rats. *The Journal of Physiology*, *165*(2), 227–245.

Banghart, M., Borges, K., Isacoff, E., Trauner, D., & Kramer, R. H. (2004). Light-activated ion channels for remote control of neuronal firing. *Nature Neuroscience*, *7*(12), 1381–1386.

Baver, S. B., Hope, K., Guyot, S., Bjørbaek, C., Kaczorowski, C., & O'Connell, K. M.

S. (2014). Leptin modulates the intrinsic excitability of AgRP/NPY neurons in the arcuate nucleus of the hypothalamus. *The Journal of Neuroscience: The Official Journal of the Society for Neuroscience*, *34*(16), 5486–5496.

Beaulieu, J.-M., & Gainetdinov, R. R. (2011). The physiology, signaling, and pharmacology of dopamine receptors. *Pharmacological Reviews*, *63*(1), 182–217.

Bermeo, K., Castro, H., Arenas, I., & Garcia, D. E. (2020). AMPK mediates regulation of voltage-gated calcium channels by leptin in isolated neurons from arcuate nucleus. *American Journal of Physiology. Endocrinology and Metabolism*, *319*(6), E1112–E1120.

Berridge, K. C., & Aldridge, J. W. (2008). DECISION UTILITY, THE BRAIN, AND PURSUIT OF HEDONIC GOALS. *Social Cognition*, *26*(5), 621–646.

Berridge, K. C., Ho, C.-Y., Richard, J. M., & DiFeliceantonio, A. G. (2010). The tempted brain eats: pleasure and desire circuits in obesity and eating disorders. *Brain Research*, *1350*, 43–64.

Berrios, J., Li, C., Madara, J. C., Garfield, A. S., Steger, J. S., Krashes, M. J., & Lowell, B. B. (2021). Food cue regulation of AGRP hunger neurons guides learning. *Nature*, 1–6.

Betley, J. N., Cao, Z. F. H., Ritola, K. D., & Sternson, S. M. (2013). Parallel, redundant circuit organization for homeostatic control of feeding behavior. *Cell*, *155*(6), 1337–1350.

Beutler, L. R., Chen, Y., Ahn, J. S., Lin, Y.-C., Essner, R. A., & Knight, Z. A. (2017).

Dynamics of Gut-Brain Communication Underlying Hunger. *Neuron*, *96*(2), 461–475.e5.

Bhaskaran, K., Douglas, I., Forbes, H., dos-Santos-Silva, I., Leon, D. A., & Smeeth, L. (2014). Body-mass index and risk of 22 specific cancers: a population-based cohort study of 5·24 million UK adults. *The Lancet*, *384*(9945), 755–765.

Bhaskar, S., Hemavathy, D., & Prasad, S. (2016). Prevalence of chronic insomnia in adult patients and its correlation with medical comorbidities. *Journal of Family Medicine and Primary Care*, *5*(4), 780–784.

Borgmann, D., Ciglieri, E., Biglari, N., Brandt, C., Cremer, A. L., Backes, H., Tittgemeyer, M., Wunderlich, F. T., Brüning, J. C., & Fenselau, H. (2021). Gut-brain communication by distinct sensory neurons differently controls feeding and glucose metabolism. *Cell Metabolism*, *33*(7), 1466–1482.e7.

Bouret, S. G., Bates, S. H., Chen, S., Myers, M. G., Jr, & Simerly, R. B. (2012). Distinct roles for specific leptin receptor signals in the development of hypothalamic feeding circuits. *The Journal of Neuroscience: The Official Journal of the Society for Neuroscience*, *32*(4), 1244–1252.

Boyden, E. S., Zhang, F., Bamberg, E., Nagel, G., & Deisseroth, K. (2005). Millisecond-timescale, genetically targeted optical control of neural activity. *Nature Neuroscience*, *8*(9), 1263–1268.

Buhr, E. D., & Takahashi, J. S. (2013). Molecular components of the Mammalian circadian clock. *Handbook of Experimental Pharmacology*, *217*, 3–27.

Buijs, F. N., Guzmán-Ruiz, M., León-Mercado, L., Basualdo, M. C., Escobar, C., Kalsbeek, A., & Buijs, R. M. (2017). Suprachiasmatic Nucleus Interaction with the Arcuate Nucleus; Essential for Organizing Physiological Rhythms. *eNeuro*, *4*(2). https://doi.org/10.1523/ENEURO.0028-17.2017

Buijs, R. M., Scheer, F. A., Kreier, F., Yi, C., Bos, N., Goncharuk, V. D., & Kalsbeek, A. (2006). Organization of circadian functions: interaction with the body. *Progress in Brain Research*, *153*, 341–360.

Bultman, S. J., Michaud, E. J., & Woychik, R. P. (1992). Molecular characterization of the mouse agouti locus. *Cell*, *71*(7), 1195–1204.

Cahill, E., Pascoli, V., Trifilieff, P., Savoldi, D., Kappès, V., Lüscher, C., Caboche, J., & Vanhoutte, P. (2014). D1R/GluN1 complexes in the striatum integrate dopamine and glutamate signalling to control synaptic plasticity and cocaine-induced responses. *Molecular Psychiatry*, *19*(12), 1295–1304.

Cammisotto, P. G., Renaud, C., Gingras, D., Delvin, E., Levy, E., & Bendayan, M. (2005). Endocrine and exocrine secretion of leptin by the gastric mucosa. *The Journal of Histochemistry and Cytochemistry: Official Journal of the Histochemistry Society*, *53*(7), 851–860.

Campbell, J. N., Macosko, E. Z., Fenselau, H., Pers, T. H., Lyubetskaya, A., Tenen, D., Goldman, M., Verstegen, A. M. J., Resch, J. M., McCarroll, S. A., Rosen, E. D., Lowell, B. B., & Tsai, L. T. (2017). A molecular census of arcuate hypothalamus and median eminence cell types. *Nature Neuroscience*, *20*(3), 484–496.

Cawley, J., & Meyerhoefer, C. (2012). The medical care costs of obesity: an instrumental variables approach. *Journal of Health Economics*, *31*(1), 219–230.

Chaix, A., Deota, S., Bhardwaj, R., Lin, T., & Panda, S. (2021). Sex- and age-dependent outcomes of 9-hour time-restricted feeding of a Western high-fat high-sucrose diet in C57BL/6J mice. *Cell Reports*, *36*(7), 109543.

Chen, S.-R., Chen, H., Zhou, J.-J., Pradhan, G., Sun, Y., Pan, H.-L., & Li, D.-P. (2017). Ghrelin receptors mediate ghrelin-induced excitation of agouti-related protein/neuropeptide Y but not pro-opiomelanocortin neurons. *Journal of Neurochemistry*, *142*(4), 512–520.

Chen, Y., Essner, R. A., Kosar, S., Miller, O. H., Lin, Y.-C., Mesgarzadeh, S., & Knight, Z. A. (2019). Sustained NPY signaling enables AgRP neurons to drive feeding. *eLife*, *8*. https://doi.org/10.7554/eLife.46348

Chen, Y., Lin, Y.-C., Kuo, T.-W., & Knight, Z. A. (2015). Sensory detection of food rapidly modulates arcuate feeding circuits. *Cell*, *160*(5), 829–841.

Chen, Z. (2019). Temporal Control of Appetite by AgRP Clocks [Review of *Temporal Control of Appetite by AgRP Clocks*]. *Cell Metabolism*, *29*(5), 1022–1023.

Claret, M., Smith, M. A., Batterham, R. L., Selman, C., Choudhury, A. I., Fryer, L. G. D., Clements, M., Al-Qassab, H., Heffron, H., Xu, A. W., Speakman, J. R., Barsh, G. S., Viollet, B., Vaulont, S., Ashford, M. L. J., Carling, D., & Withers, D. J. (2007). AMPK is essential for energy homeostasis regulation and glucose sensing by POMC and AgRP neurons. *The Journal of Clinical Investigation*, *117*(8), 2325–

2336.

Cloues, R. K., & Sather, W. A. (2003). Afterhyperpolarization regulates firing rate in neurons of the suprachiasmatic nucleus. *The Journal of Neuroscience: The Official Journal of the Society for Neuroscience*, *23*(5), 1593–1604.

Colten, H. R., Altevogt, B. M., & Institute of Medicine (US) Committee on Sleep Medicine and Research. (2006). *Extent and Health Consequences of Chronic Sleep Loss and Sleep Disorders*. National Academies Press (US).

Cone, R. D., Cowley, M. A., Butler, A. A., Fan, W., Marks, D. L., & Low, M. J. (2001). The arcuate nucleus as a conduit for diverse signals relevant to energy homeostasis. *International Journal of Obesity and Related Metabolic Disorders: Journal of the International Association for the Study of Obesity*, *25 Suppl 5*, S63–S67.

Cowley, M. A., Smart, J. L., Rubinstein, M., Cerdán, M. G., Diano, S., Horvath, T. L., Cone, R. D., & Low, M. J. (2001). Leptin activates anorexigenic POMC neurons through a neural network in the arcuate nucleus. *Nature*, *411*(6836), 480–484.

Cowley, M. A., Smith, R. G., Diano, S., Tschöp, M., Pronchuk, N., Grove, K. L., Strasburger, C. J., Bidlingmaier, M., Esterman, M., Heiman, M. L., Garcia-Segura, L. M., Nillni, E. A., Mendez, P., Low, M. J., Sotonyi, P., Friedman, J. M., Liu, H., Pinto, S., Colmers, W. F., … Horvath, T. L. (2003). The distribution and mechanism of action of ghrelin in the CNS demonstrates a novel hypothalamic circuit regulating energy homeostasis. *Neuron*, *37*(4), 649–661.

Dietrich, M. O., Antunes, C., Geliang, G., Liu, Z.-W., Borok, E., Nie, Y., Xu, A. W., Souza, D. O., Gao, Q., Diano, S., Gao, X.-B., & Horvath, T. L. (2010). Agrp neurons mediate Sirt1's action on the melanocortin system and energy balance: roles for Sirt1 in neuronal firing and synaptic plasticity. *The Journal of Neuroscience: The Official Journal of the Society for Neuroscience*, *30*(35), 11815–11825.

Dietrich, M. O., & Horvath, T. L. (2013). Hypothalamic control of energy balance: insights into the role of synaptic plasticity. *Trends in Neurosciences*, *36*(2), 65–73.

Doghramji, K. (2007). Melatonin and its receptors: a new class of sleep-promoting agents. *Journal of Clinical Sleep Medicine: JCSM: Official Publication of the American Academy of Sleep Medicine*, *3*(5 Suppl), S17–S23.

Engin, A. (2017). The Definition and Prevalence of Obesity and Metabolic Syndrome. In A. B. Engin & A. Engin (Eds.), *Obesity and Lipotoxicity* (pp. 1–17). Springer International Publishing.

Evans, J. A., & Davidson, A. J. (2013). Health consequences of circadian disruption in humans and animal models. *Progress in Molecular Biology and Translational Science*, *119*, 283–323.

Ewbank, S. N., Campos, C. A., Chen, J. Y., Bowen, A. J., Padilla, S. L., Dempsey, J. L., Cui, J. Y., & Palmiter, R. D. (2020). Chronic Gq signaling in AgRP neurons does not cause obesity. *Proceedings of the National Academy of Sciences of the United States of America*, *117*(34), 20874–20880.

Fan, J., Zeng, H., Olson, D. P., Huber, K. M., Gibson, J. R., & Takahashi, J. S.

(2015). Vasoactive intestinal polypeptide (VIP)-expressing neurons in the suprachiasmatic nucleus provide sparse GABAergic outputs to local neurons with circadian regulation occurring distal to the opening of postsynaptic GABAA ionotropic receptors. *The Journal of Neuroscience: The Official Journal of the Society for Neuroscience*, *35*(5), 1905–1920.

Fan, W., Boston, B. A., Kesterson, R. A., Hruby, V. J., & Cone, R. D. (1997). Role of melanocortinergic neurons in feeding and the agouti obesity syndrome. *Nature*, *385*(6612), 165–168.

Fitzgerald, P., & Dinan, T. G. (2008). Prolactin and dopamine: what is the connection? A review article. *Journal of Psychopharmacology* , *22*(2 Suppl), 12–19.

Frederick, A. L., Yano, H., Trifilieff, P., Vishwasrao, H. D., Biezonski, D., Mészáros, J., Urizar, E., Sibley, D. R., Kellendonk, C., Sonntag, K. C., Graham, D. L., Colbran, R. J., Stanwood, G. D., & Javitch, J. A. (2015). Evidence against dopamine D1/D2 receptor heteromers. *Molecular Psychiatry*, *20*(11), 1373–1385.

Fryar, C. D., Carroll, M. D., & Afful, J. (2020). Prevalence of overweight, obesity, and severe obesity among adults aged 20 and over: United States, 1960--1962 through 2017--2018. *NCHS Health E-Stats*. http://www.publicnow.com/view/57BFCB292A6D12A9A3EE633921C052DED8F0D94B

Gao, M., Sun, Q., & Liu, Q. (2021). Mitochondrial ATP-Sensitive K+ Channel Opening Increased the Airway Smooth Muscle Cell Proliferation by Activating the

PI3K/AKT Signaling Pathway in a Rat Model of Asthma. *Canadian Respiratory Journal: Journal of the Canadian Thoracic Society*, *2021*, 8899878.

Gao, Y., Yao, T., Deng, Z., Sohn, J.-W., Sun, J., Huang, Y., Kong, X., Yu, K.-J., Wang, R.-T., Chen, H., Guo, H., Yan, J., Cunningham, K. A., Chang, Y., Liu, T., & Williams, K. W. (2017). TrpC5 Mediates Acute Leptin and Serotonin Effects via Pomc Neurons. *Cell Reports*, *18*(3), 583–592.

Garfield, A. S., Shah, B. P., Burgess, C. R., Li, M. M., Li, C., Steger, J. S., Madara, J. C., Campbell, J. N., Kroeger, D., Scammell, T. E., Tannous, B. A., Myers, M. G., Jr, Andermann, M. L., Krashes, M. J., & Lowell, B. B. (2016). Dynamic GABAergic afferent modulation of AgRP neurons. *Nature Neuroscience*, *19*(12), 1628–1635.

Gizowski, C., Zaelzer, C., & Bourque, C. W. (2016). Clock-driven vasopressin neurotransmission mediates anticipatory thirst prior to sleep. *Nature*, *537*(7622), 685–688.

Gizowski, C., Zaelzer, C., & Bourque, C. W. (2018). Activation of organum vasculosum neurons and water intake in mice by vasopressin neurons in the suprachiasmatic nucleus. *Journal of Neuroendocrinology*. https://doi.org/10.1111/jne.12577

Glaum, S. R., Hara, M., Bindokas, V. P., Lee, C. C., Polonsky, K. S., Bell, G. I., & Miller, R. J. (1996). Leptin, the obese gene product, rapidly modulates synaptic transmission in the hypothalamus. *Molecular Pharmacology*, *50*(2), 230–235.

Goldstein, N., McKnight, A. D., Carty, J. R. E., Arnold, M., Betley, J. N., & Alhadeff,

A. L. (2021). Hypothalamic detection of macronutrients via multiple gut-brain pathways. *Cell Metabolism*, *33*(3), 676–687.e5.

Grippo, R. M., Purohit, A. M., Zhang, Q., Zweifel, L. S., & Güler, A. D. (2017). Direct Midbrain Dopamine Input to the Suprachiasmatic Nucleus Accelerates Circadian Entrainment. *Current Biology: CB*, *27*(16), 2465–2475.e3.

Grippo, R. M., Tang, Q., Zhang, Q., Chadwick, S. R., Gao, Y., Altherr, E. B., Sipe, L., Purohit, A. M., Purohit, N. M., Sunkara, M. D., Cios, K. J., Sidikpramana, M., Spano, A. J., Campbell, J. N., Steele, A. D., Hirsh, J., Deppmann, C. D., Wu, M., Scott, M. M., & Güler, A. D. (2020). Dopamine Signaling in the Suprachiasmatic Nucleus Enables Weight Gain Associated with Hedonic Feeding. *Current Biology: CB*, *30*(2), 196–208.e8.

Gropp, E., Shanabrough, M., Borok, E., Xu, A. W., Janoschek, R., Buch, T., Plum, L., Balthasar, N., Hampel, B., Waisman, A., Barsh, G. S., Horvath, T. L., & Brüning, J. C. (2005). Agouti-related peptide-expressing neurons are mandatory for feeding. *Nature Neuroscience*, *8*(10), 1289–1291.

Guilding, C., Hughes, A. T. L., Brown, T. M., Namvar, S., & Piggins, H. D. (2009). A riot of rhythms: neuronal and glial circadian oscillators in the mediobasal hypothalamus. *Molecular Brain*, *2*(1), 1–19.

Hannibal, J., Georg, B., & Fahrenkrug, J. (2017). PAC1- and VPAC2 receptors in light regulated behavior and physiology: Studies in single and double mutant mice. *PloS One*, *12*(11), e0188166.

Han, Y., Xia, G., & Wu, Q. (2018). Functional Interrogation of the AgRP Neural Circuits in Control of Appetite, Body Weight, and Behaviors. In Q. Wu & R. Zheng (Eds.), *Neural Regulation of Metabolism* (pp. 1–16). Springer Singapore.

Harding, C., Bechtold, D. A., & Brown, T. M. (2020). Suprachiasmatic nucleus-dependent and independent outputs driving rhythmic activity in hypothalamic and thalamic neurons. *BMC Biology*, *18*(1), 134.

Hastings, M. H., Duffield, G. E., Ebling, F. J., Kidd, A., Maywood, E. S., & Schurov, I. (1997). Non-photic signalling in the suprachiasmatic nucleus. *Biology of the Cell / under the Auspices of the European Cell Biology Organization*, *89*(8), 495–503.

Hattar, S., Kumar, M., Park, A., Tong, P., Tung, J., Yau, K.-W., & Berson, D. M. (2006). Central projections of melanopsin-expressing retinal ganglion cells in the mouse. *The Journal of Comparative Neurology*, *497*(3), 326–349.

Hermanstyne, T. O., Simms, C. L., Carrasquillo, Y., Herzog, E. D., & Nerbonne, J. M. (2016). Distinct Firing Properties of Vasoactive Intestinal Peptide-Expressing Neurons in the Suprachiasmatic Nucleus. *Journal of Biological Rhythms*, *31*(1), 57–67.

Hernández-López, S., Bargas, J., Surmeier, D. J., Reyes, A., & Galarraga, E. (1997). D1 receptor activation enhances evoked discharge in neostriatal medium spiny neurons by modulating an L-type Ca2+ conductance. *The Journal of Neuroscience: The Official Journal of the Society for Neuroscience*, *17*(9), 3334–3342.

Herzog, E. D. (2007). Neurons and networks in daily rhythms. *Nature Reviews. Neuroscience*, *8*(10), 790–802.

Herzog, E. D., Hermanstyne, T., Smyllie, N. J., & Hastings, M. H. (2017). Regulating the Suprachiasmatic Nucleus (SCN) Circadian Clockwork: Interplay between Cell-Autonomous and Circuit-Level Mechanisms. *Cold Spring Harbor Perspectives in Biology*, *9*(1). https://doi.org/10.1101/cshperspect.a027706

Heusner, C. L., Beutler, L. R., Houser, C. R., & Palmiter, R. D. (2008). Deletion of GAD67 in dopamine receptor-1 expressing cells causes specific motor deficits. *Genesis* , *46*(7), 357–367.

Hewson, A. K., Tung, L. Y. C., Connell, D. W., Tookman, L., & Dickson, S. L. (2002). The rat arcuate nucleus integrates peripheral signals provided by leptin, insulin, and a ghrelin mimetic. *Diabetes*, *51*(12), 3412–3419.

Hill, J. O., Wyatt, H. R., & Peters, J. C. (2013). The Importance of Energy Balance. *European Endocrinology*, *9*(2), 111–115.

Hill, J. W., Williams, K. W., Ye, C., Luo, J., Balthasar, N., Coppari, R., Cowley, M. A., Cantley, L. C., Lowell, B. B., & Elmquist, J. K. (2008). Acute effects of leptin require PI3K signaling in hypothalamic proopiomelanocortin neurons in mice. *The Journal of Clinical Investigation*, *118*(5), 1796–1805.

Hirabayashi, T., Nakamachi, T., & Shioda, S. (2018). Discovery of PACAP and its receptors in the brain. *The Journal of Headache and Pain*, *19*(1), 28.

Huszar, D., Lynch, C. A., Fairchild-Huntress, V., Dunmore, J. H., Fang, Q.,

Berkemeier, L. R., Gu, W., Kesterson, R. A., Boston, B. A., Cone, R. D., Smith, F. J., Campfield, L. A., Burn, P., & Lee, F. (1997). Targeted disruption of the melanocortin-4 receptor results in obesity in mice. *Cell*, *88*(1), 131–141.

Illius, A. W., Tolkamp, B. J., & Yearsley, J. (2002). The evolution of the control of food intake. *The Proceedings of the Nutrition Society*, *61*(4), 465–472.

Iserentant, H., Peelman, F., Defeau, D., Vandekerckhove, J., Zabeau, L., & Tavernier, J. (2005). Mapping of the interface between leptin and the leptin receptor CRH2 domain. *Journal of Cell Science*, *118*(Pt 11), 2519–2527.

Iversen, S., Iversen, L., & Saper, C. B. (2000). The autonomic nervous system and the hypothalamus. *Principles of Neural Science*, *4*, 960–981.

Jackson, A. C., Yao, G. L., & Bean, B. P. (2004). Mechanism of spontaneous firing in dorsomedial suprachiasmatic nucleus neurons. *The Journal of Neuroscience: The Official Journal of the Society for Neuroscience*, *24*(37), 7985–7998.

Jais, A., Paeger, L., Sotelo-Hitschfeld, T., Bremser, S., Prinzensteiner, M., Klemm, P., Mykytiuk, V., Widdershooven, P. J. M., Vesting, A. J., Grzelka, K., Minère, M., Cremer, A. L., Xu, J., Korotkova, T., Lowell, B. B., Zeilhofer, H. U., Backes, H., Fenselau, H., Wunderlich, F. T., … Brüning, J. C. (2020). PNOCARC Neurons Promote Hyperphagia and Obesity upon High-Fat-Diet Feeding. *Neuron*, *106*(6), 1009–1025.e10.

Johnson, P. M., & Kenny, P. J. (2010). Dopamine D2 receptors in addiction-like reward dysfunction and compulsive eating in obese rats. *Nature Neuroscience*,

13(5), 635–641.

Jones, E. S., Nunn, N., Chambers, A. P., Østergaard, S., Wulff, B. S., & Luckman, S. M. (2019). Modified Peptide YY Molecule Attenuates the Activity of NPY/AgRP Neurons and Reduces Food Intake in Male Mice. *Endocrinology*, *160*(11), 2737–2747.

Jones, J. R., Tackenberg, M. C., & McMahon, D. G. (2015). Manipulating circadian clock neuron firing rate resets molecular circadian rhythms and behavior. *Nature Neuroscience*, *18*(3), 373–375.

Kalsbeek, A., Palm, I. F., La Fleur, S. E., Scheer, F. A. J. L., Perreau-Lenz, S., Ruiter, M., Kreier, F., Cailotto, C., & Buijs, R. M. (2006). SCN outputs and the hypothalamic balance of life. *Journal of Biological Rhythms*, *21*(6), 458–469.

Kearney, J. (2010). Food consumption trends and drivers. *Philosophical Transactions of the Royal Society of London. Series B, Biological Sciences*, *365*(1554), 2793–2807.

Kim, P., Oster, H., Lehnert, H., Schmid, S. M., Salamat, N., Barclay, J. L., Maronde, E., Inder, W., & Rawashdeh, O. (2019). Coupling the Circadian Clock to Homeostasis: The Role of Period in Timing Physiology. *Endocrine Reviews*, *40*(1), 66–95.

Koch, C. E., Begemann, K., Kiehn, J. T., Griewahn, L., Mauer, J., M E Hess, Moser, A., Schmid, S. M., Brüning, J. C., & Oster, H. (2020). Circadian regulation of hedonic appetite in mice by clocks in dopaminergic neurons of the VTA. *Nature*

Communications, *11*(1), 3071.

Kohno, D., & Yada, T. (2012). Arcuate NPY neurons sense and integrate peripheral metabolic signals to control feeding. *Neuropeptides*, *46*(6), 315–319.

Krashes, M. J., Koda, S., Ye, C., Rogan, S. C., Adams, A. C., Cusher, D. S., Maratos-Flier, E., Roth, B. L., & Lowell, B. B. (2011). Rapid, reversible activation of AgRP neurons drives feeding behavior in mice. *The Journal of Clinical Investigation*, *121*(4), 1424–1428.

Krashes, M. J., Shah, B. P., Koda, S., & Lowell, B. B. (2013). Rapid versus delayed stimulation of feeding by the endogenously released AgRP neuron mediators GABA, NPY, and AgRP. *Cell Metabolism*, *18*(4), 588–595.

Kudo, T., Tahara, Y., Gamble, K. L., McMahon, D. G., Block, G. D., & Colwell, C. S. (2013). Vasoactive intestinal peptide produces long-lasting changes in neural activity in the suprachiasmatic nucleus. *Journal of Neurophysiology*, *110*(5), 1097–1106.

Lahiri, A. K., & Bevan, M. D. (2020). Dopaminergic Transmission Rapidly and Persistently Enhances Excitability of D1 Receptor-Expressing Striatal Projection Neurons. *Neuron*, *106*(2), 277–290.e6.

Laing, B. T., Li, P., Schmidt, C. A., Bunner, W., Yuan, Y., Landry, T., Prete, A., McClung, J. M., & Huang, H. (2018). AgRP/NPY Neuron Excitability Is Modulated by Metabotropic Glutamate Receptor 1 During Fasting. *Frontiers in Cellular Neuroscience*, *12*, 276.

Leib, D. E., Zimmerman, C. A., & Knight, Z. A. (2016). Thirst. *Current Biology: CB*, *26*(24), R1260–R1265.

LeSauter, J., Silver, R., Cloues, R., & Witkovsky, P. (2011). Light exposure induces short- and long-term changes in the excitability of retinorecipient neurons in suprachiasmatic nucleus. *Journal of Neurophysiology*, *106*(2), 576–588.

Liu, T., Kong, D., Shah, B. P., Ye, C., Koda, S., Saunders, A., Ding, J. B., Yang, Z., Sabatini, B. L., & Lowell, B. B. (2012). Fasting activation of AgRP neurons requires NMDA receptors and involves spinogenesis and increased excitatory tone. *Neuron*, *73*(3), 511–522.

Li, Y., Zhang, X., Winkelman, J. W., Redline, S., Hu, F. B., Stampfer, M., Ma, J., & Gao, X. (2014). Association between insomnia symptoms and mortality: a prospective study of U.S. men. *Circulation*, *129*(7), 737–746.

Lu, D., Willard, D., Patel, I. R., Kadwell, S., Overton, L., Kost, T., Luther, M., Chen, W., Woychik, R. P., & Wilkison, W. O. (1994). Agouti protein is an antagonist of the melanocyte-stimulating-hormone receptor. *Nature*, *371*(6500), 799–802.

Luo, S. X., Huang, J., Li, Q., Mohammad, H., Lee, C.-Y., Krishna, K., Kok, A. M.-Y., Tan, Y. L., Lim, J. Y., Li, H., Yeow, L. Y., Sun, J., He, M., Grandjean, J., Sajikumar, S., Han, W., & Fu, Y. (2018). Regulation of feeding by somatostatin neurons in the tuberal nucleus. *Science*, *361*(6397), 76–81.

Luo, Y.-J., Li, Y.-D., Wang, L., Yang, S.-R., Yuan, X.-S., Wang, J., Cherasse, Y., Lazarus, M., Chen, J.-F., Qu, W.-M., & Huang, Z.-L. (2018). Nucleus accumbens

controls wakefulness by a subpopulation of neurons expressing dopamine D1 receptors. *Nature Communications*, *9*(1), 1576.

Luquet, S., Perez, F. A., Hnasko, T. S., & Palmiter, R. D. (2005). NPY/AgRP neurons are essential for feeding in adult mice but can be ablated in neonates. *Science*, *310*(5748), 683–685.

Madisen, L., Zwingman, T. A., Sunkin, S. M., Oh, S. W., Zariwala, H. A., Gu, H., Ng, L. L., Palmiter, R. D., Hawrylycz, M. J., Jones, A. R., Lein, E. S., & Zeng, H. (2010). A robust and high-throughput Cre reporting and characterization system for the whole mouse brain. *Nature Neuroscience*, *13*(1), 133–140.

Mandelblat-Cerf, Y., Ramesh, R. N., Burgess, C. R., Patella, P., Yang, Z., Lowell, B. B., & Andermann, M. L. (2015). Arcuate hypothalamic AgRP and putative POMC neurons show opposite changes in spiking across multiple timescales. *eLife*, *4*. https://doi.org/10.7554/eLife.07122

Mann, T., Tomiyama, A. J., Westling, E., Lew, A.-M., Samuels, B., & Chatman, J. (2007). Medicare's search for effective obesity treatments: diets are not the answer. *The American Psychologist*, *62*(3), 220–233.

Manvich, D. F., Webster, K. A., Foster, S. L., Farrell, M. S., Ritchie, J. C., Porter, J. H., & Weinshenker, D. (2018). The DREADD agonist clozapine N-oxide (CNO) is reverse-metabolized to clozapine and produces clozapine-like interoceptive stimulus effects in rats and mice. *Scientific Reports*, *8*(1), 3840.

Mazuski, C., Abel, J. H., Chen, S. P., Hermanstyne, T. O., Jones, J. R., Simon, T.,

Doyle, F. J., 3rd, & Herzog, E. D. (2018). Entrainment of Circadian Rhythms Depends on Firing Rates and Neuropeptide Release of VIP SCN Neurons. *Neuron*, *99*(3), 555–563.e5.

Mazzone, C. M., Liang-Guallpa, J., Li, C., Wolcott, N. S., Boone, M. H., Southern, M., Kobzar, N. P., Salgado, I. de A., Reddy, D. M., Sun, F., Zhang, Y., Li, Y., Cui, G., & Krashes, M. J. (2020). High-fat food biases hypothalamic and mesolimbic expression of consummatory drives. *Nature Neuroscience*, *23*(10), 1253–1266.

McNeill, D. S., Sheely, C. J., Ecker, J. L., Badea, T. C., Morhardt, D., Guido, W., & Hattar, S. (2011). Development of melanopsin-based irradiance detecting circuitry. *Neural Development*, *6*, 8.

Miller, M. W., Duhl, D. M., Vrieling, H., Cordes, S. P., Ollmann, M. M., Winkes, B. M., & Barsh, G. S. (1993). Cloning of the mouse agouti gene predicts a secreted protein ubiquitously expressed in mice carrying the lethal yellow mutation. *Genes & Development*, *7*(3), 454–467.

Miller, N. E. (1960). Motivational effects of brain stimulation and drugs. *Federation Proceedings*, *19*, 846–854.

Miller, S. M., Marcotulli, D., Shen, A., & Zweifel, L. S. (2019). Divergent medial amygdala projections regulate approach-avoidance conflict behavior. *Nature Neuroscience*, *22*(4), 565–575.

Mirshamsi, S., Laidlaw, H. A., Ning, K., Anderson, E., Burgess, L. A., Gray, A., Sutherland, C., & Ashford, M. L. J. (2004). Leptin and insulin stimulation of

signalling pathways in arcuate nucleus neurones: PI3K dependent actin reorganization and KATP channel activation. *BMC Neuroscience*, *5*, 54.

Missale, C., Nash, S. R., Robinson, S. W., Jaber, M., & Caron, M. G. (1998). Dopamine receptors: from structure to function. *Physiological Reviews*, *78*(1), 189–225.

Mistlberger, R. E. (2011). Neurobiology of food anticipatory circadian rhythms. *Physiology & Behavior*, *104*(4), 535–545.

Mohawk, J. A., Baer, M. L., & Menaker, M. (2009). The methamphetamine-sensitive circadian oscillator does not employ canonical clock genes. *Proceedings of the National Academy of Sciences of the United States of America*, *106*(9), 3519–3524.

Moore, R. Y. (1995). Organization of the mammalian circadian system. *Ciba Foundation Symposium*, *183*, 88–99; discussion 100–106.

Moore, R. Y., & Speh, J. C. (1993). GABA is the principal neurotransmitter of the circadian system. *Neuroscience Letters*, *150*(1), 112–116.

Moore, R. Y., Speh, J. C., & Leak, R. K. (2002). Suprachiasmatic nucleus organization. *Cell and Tissue Research*, *309*(1), 89–98.

Morrison, S. D., & Mayer, J. (1957). Effect of sham operations in the hypothalamus on food and water intake of the rat. *The American Journal of Physiology*, *191*(2), 255–258.

Mrosovsky, N., Reebs, S. G., Honrado, G. I., & Salmon, P. A. (1989). Behavioural

entrainment of circadian rhythms. *Experientia*, *45*(8), 696–702.

Müller, T. D., Nogueiras, R., Andermann, M. L., Andrews, Z. B., Anker, S. D., Argente, J., Batterham, R. L., Benoit, S. C., Bowers, C. Y., Broglio, F., Casanueva, F. F., D'Alessio, D., Depoortere, I., Geliebter, A., Ghigo, E., Cole, P. A., Cowley, M., Cummings, D. E., Dagher, A., … Tschöp, M. H. (2015). Ghrelin. *Molecular Metabolism*, *4*(6), 437–460.

Münzberg, H., & Morrison, C. D. (2015). Structure, production and signaling of leptin. *Metabolism: Clinical and Experimental*, *64*(1), 13–23.

Muoio, D. M., & Lynis Dohm, G. (2002). Peripheral metabolic actions of leptin. *Best Practice & Research. Clinical Endocrinology & Metabolism*, *16*(4), 653–666.

Nakahata, Y., Yoshida, M., Takano, A., Soma, H., Yamamoto, T., Yasuda, A., Nakatsu, T., & Takumi, T. (2008). A direct repeat of E-box-like elements is required for cell-autonomous circadian rhythm of clock genes. *BMC Molecular Biology*, *9*, 1.

Nakajima, K.-I., Cui, Z., Li, C., Meister, J., Cui, Y., Fu, O., Smith, A. S., Jain, S., Lowell, B. B., Krashes, M. J., & Wess, J. (2016). Gs-coupled GPCR signalling in AgRP neurons triggers sustained increase in food intake. *Nature Communications*, *7*, 10268.

Ni, Y., Chen, Q., Cai, J., Xiao, L., & Zhang, J. (2021). Three lactation-related hormones: Regulation of hypothalamus-pituitary axis and function on lactation. *Molecular and Cellular Endocrinology*, *520*, 111084.

Noe, M. (2021). firing threshold value from an action potential phase plot.

Mathworks Central Answers. https://www.mathworks.com/matlabcentral/answers/733193-how-do-i-extract-the-firing-threshold-value-from-an-action-potential-phase-plot

Nour, N. N. (2010). Obesity in resource-poor nations. *Reviews in Obstetrics and Gynecology*, *3*(4), 180–184.

O'Dowd, B. F., Ji, X., Nguyen, T., & George, S. R. (2012). Two amino acids in each of D1 and D2 dopamine receptor cytoplasmic regions are involved in D1-D2 heteromer formation. *Biochemical and Biophysical Research Communications*, *417*(1), 23–28.

Ogden, C. L., Fryar, C. D., Martin, C. B., Freedman, D. S., Carroll, M. D., Gu, Q., & Hales, C. M. (2020). Trends in Obesity Prevalence by Race and Hispanic Origin—1999-2000 to 2017-2018. *JAMA: The Journal of the American Medical Association*, *324*(12), 1208–1210.

Okamoto-Mizuno, K., & Mizuno, K. (2012). Effects of thermal environment on sleep and circadian rhythm. *Journal of Physiological Anthropology*, *31*, 14.

Okamura, H., Bérod, A., Julien, J. F., Geffard, M., Kitahama, K., Mallet, J., & Bobillier, P. (1989). Demonstration of GABAergic cell bodies in the suprachiasmatic nucleus: in situ hybridization of glutamic acid decarboxylase (GAD) mRNA and immunocytochemistry of GAD and GABA. *Neuroscience Letters*, *102*(2-3), 131–136.

O'Neill, J. S., Maywood, E. S., & Hastings, M. H. (2013). Cellular Mechanisms of

Circadian Pacemaking: Beyond Transcriptional Loops. In A. Kramer & M. Merrow (Eds.), *Circadian Clocks* (pp. 67–103). Springer Berlin Heidelberg.

Palmiter, R. D. (2007). Is dopamine a physiologically relevant mediator of feeding behavior? *Trends in Neurosciences*, *30*(8), 375–381.

Park, H.-K., & Ahima, R. S. (2014). Leptin signaling. *F1000prime Reports*, *6*, 73.

Parthasarathy, S., Vasquez, M. M., Halonen, M., Bootzin, R., Quan, S. F., Martinez, F. D., & Guerra, S. (2015). Persistent insomnia is associated with mortality risk. *The American Journal of Medicine*, *128*(3), 268–275.e2.

Patriarchi, T., Cho, J. R., Merten, K., Howe, M. W., Marley, A., Xiong, W.-H., Folk, R. W., Broussard, G. J., Liang, R., Jang, M. J., Zhong, H., Dombeck, D., von Zastrow, M., Nimmerjahn, A., Gradinaru, V., Williams, J. T., & Tian, L. (2018). Ultrafast neuronal imaging of dopamine dynamics with designed genetically encoded sensors. *Science*, *360*(6396). https://doi.org/10.1126/science.aat4422

Patton, A. P., Edwards, M. D., Smyllie, N. J., Hamnett, R., Chesham, J. E., Brancaccio, M., Maywood, E. S., & Hastings, M. H. (2020). The VIP-VPAC2 neuropeptidergic axis is a cellular pacemaking hub of the suprachiasmatic nucleus circadian circuit. *Nature Communications*, *11*(1), 3394.

Paulson, P. E., Camp, D. M., & Robinson, T. E. (1991). Time course of transient behavioral depression and persistent behavioral sensitization in relation to regional brain monoamine concentrations during amphetamine withdrawal in rats. *Psychopharmacology*, *103*(4), 480–492.

Petreanu, L., Huber, D., Sobczyk, A., & Svoboda, K. (2007). Channelrhodopsin-2-assisted circuit mapping of long-range callosal projections. *Nature Neuroscience*, *10*(5), 663–668.

Powell-Wiley, T. M., Poirier, P., Burke, L. E., Després, J.-P., Gordon-Larsen, P., Lavie, C. J., Lear, S. A., Ndumele, C. E., Neeland, I. J., Sanders, P., St-Onge, M.-P., & American Heart Association Council on Lifestyle and Cardiometabolic Health; Council on Cardiovascular and Stroke Nursing; Council on Clinical Cardiology; Council on Epidemiology and Prevention; and Stroke Council. (2021). Obesity and Cardiovascular Disease: A Scientific Statement From the American Heart Association. *Circulation*, *143*(21), e984–e1010.

Power, A., Hughes, A. T. L., Samuels, R. E., & Piggins, H. D. (2010). Rhythm-promoting actions of exercise in mice with deficient neuropeptide signaling. *Journal of Biological Rhythms*, *25*(4), 235–246.

Qiu, J., Fang, Y., Rønnekleiv, O. K., & Kelly, M. J. (2010). Leptin excites proopiomelanocortin neurons via activation of TRPC channels. *The Journal of Neuroscience: The Official Journal of the Society for Neuroscience*, *30*(4), 1560–1565.

Rivkees, S. A., & Lachowicz, J. E. (1997). Functional D1 and D5 dopamine receptors are expressed in the suprachiasmatic, supraoptic, and paraventricular nuclei of primates. *Synapse* , *26*(1), 1–10.

Robison, B. L., & Sawyer, C. H. (1987). Hypothalamic control of ovulation and

behavioral estrus in the cat. *Brain Research*, *418*(1), 41–51.

Romero-Fernandez, W., Borroto-Escuela, D. O., Vargas-Barroso, V., Narváez, M., Di Palma, M., Agnati, L. F., Larriva Sahd, J., & Fuxe, K. (2014). Dopamine D1 and D2 receptor immunoreactivities in the arcuate-median eminence complex and their link to the tubero-infundibular dopamine neurons. *European Journal of Histochemistry: EJH*, *58*(3), 2400.

Sariñana, J., Kitamura, T., Künzler, P., Sultzman, L., & Tonegawa, S. (2014). Differential roles of the dopamine 1-class receptors, D1R and D5R, in hippocampal dependent memory. *Proceedings of the National Academy of Sciences of the United States of America*, *111*(22), 8245–8250.

Schaap, J., Bos, N. P. A., de Jeu, M. T. G., Geurtsen, A. M. S., Meijer, J. H., & Pennartz, C. M. A. (1999). Neurons of the rat suprachiasmatic nucleus show a circadian rhythm in membrane properties that is lost during prolonged whole-cell recording1Published on the World Wide Web on 20 October 1998.1. *Brain Research*, *815*(1), 154–166.

Scully, T., Ettela, A., LeRoith, D., & Gallagher, E. J. (2020). Obesity, Type 2 Diabetes, and Cancer Risk. *Frontiers in Oncology*, *10*, 615375.

Sheng, J. A., Bales, N. J., Myers, S. A., Bautista, A. I., Roueinfar, M., Hale, T. M., & Handa, R. J. (2020). The Hypothalamic-Pituitary-Adrenal Axis: Development, Programming Actions of Hormones, and Maternal-Fetal Interactions. *Frontiers in Behavioral Neuroscience*, *14*, 601939.

Shuen, J. A., Chen, M., Gloss, B., & Calakos, N. (2008). Drd1a-tdTomato BAC transgenic mice for simultaneous visualization of medium spiny neurons in the direct and indirect pathways of the basal ganglia. *The Journal of Neuroscience: The Official Journal of the Society for Neuroscience*, *28*(11), 2681–2685.

Smith, K. S., Bucci, D. J., Luikart, B. W., & Mahler, S. V. (2016). DREADDS: Use and application in behavioral neuroscience. *Behavioral Neuroscience*, *130*(2), 137–155.

Smith, M. A., Katsouri, L., Virtue, S., Choudhury, A. I., Vidal-Puig, A., Ashford, M. L. J., & Withers, D. J. (2018). Calcium Channel CaV2.3 Subunits Regulate Hepatic Glucose Production by Modulating Leptin-Induced Excitation of Arcuate Pro-opiomelanocortin Neurons. *Cell Reports*, *25*(2), 278–287.e4.

Smith, O. A. (1956). Stimulation of lateral and medial hypothalamus and food intake in the rat. *Anatomical Record*, *124*, 364–365.

Smyllie, N. J., Chesham, J. E., Hamnett, R., Maywood, E. S., & Hastings, M. H. (2016). Temporally chimeric mice reveal flexibility of circadian period-setting in the suprachiasmatic nucleus. *Proceedings of the National Academy of Sciences of the United States of America*, *113*(13), 3657–3662.

Södersten, P., Eneroth, P., & Hansen, S. (1981). NEUROENDOCRINE CONTROL OF DAILY RHYTHMS IN RAT REPRODUCTIVE BEHAVIOR. In K. Fuxe, J.-Å. Gustafsson, & L. Wetterberg (Eds.), *Steroid Hormone Regulation of the Brain* (pp. 301–315). Pergamon.

Spanswick, D., Smith, M. A., Groppi, V. E., Logan, S. D., & Ashford, M. L. (1997). Leptin inhibits hypothalamic neurons by activation of ATP-sensitive potassium channels. *Nature*, *390*(6659), 521–525.

Spanswick, D., Smith, M. A., Mirshamsi, S., Routh, V. H., & Ashford, M. L. (2000). Insulin activates ATP-sensitive K+ channels in hypothalamic neurons of lean, but not obese rats. *Nature Neuroscience*, *3*(8), 757–758.

Statovci, D., Aguilera, M., MacSharry, J., & Melgar, S. (2017). The Impact of Western Diet and Nutrients on the Microbiota and Immune Response at Mucosal Interfaces. *Frontiers in Immunology*, *8*, 838.

Stephens, M. A. C., & Wand, G. (2012). Stress and the HPA axis: role of glucocorticoids in alcohol dependence. *Alcohol Research: Current Reviews*, *34*(4), 468–483.

Stephens, T. W., Basinski, M., Bristow, P. K., Bue-Valleskey, J. M., Burgett, S. G., Craft, L., Hale, J., Hoffmann, J., Hsiung, H. M., & Kriauciunas, A. (1995). The role of neuropeptide Y in the antiobesity action of the obese gene product. *Nature*, *377*(6549), 530–532.

Sternson, S. M., Nicholas Betley, J., & Cao, Z. F. H. (2013). Neural circuits and motivational processes for hunger. *Current Opinion in Neurobiology*, *23*(3), 353–360.

Su, Z., Alhadeff, A. L., & Betley, J. N. (2017). Nutritive, Post-ingestive Signals Are the Primary Regulators of AgRP Neuron Activity. *Cell Reports*, *21*(10), 2724–2736.

Takahashi, K. A., & Cone, R. D. (2005). Fasting induces a large, leptin-dependent increase in the intrinsic action potential frequency of orexigenic arcuate nucleus neuropeptide Y/Agouti-related protein neurons. *Endocrinology*, *146*(3), 1043–1047.

Takeuchi, S., Kawanai, T., Yamauchi, R., Chen, L., Miyaoka, T., Yamada, M., Asano, S., Hayata-Takano, A., Nakazawa, T., Yano, K., Horiguchi, N., Nakagawa, S., Takuma, K., Waschek, J. A., Hashimoto, H., & Ago, Y. (2020). Activation of the VPAC2 Receptor Impairs Axon Outgrowth and Decreases Dendritic Arborization in Mouse Cortical Neurons by a PKA-Dependent Mechanism. *Frontiers in Neuroscience*, *14*, 521.

Teitelbaum, P., & Stellar, E. (1954). Recovery from the failure to eat produced by hypothalamic lesions. *Science*, *120*(3126), 894–895.

Ting, J. T., Daigle, T. L., Chen, Q., & Feng, G. (2014). Acute Brain Slice Methods for Adult and Aging Animals: Application of Targeted Patch Clamp Analysis and Optogenetics. In M. Martina & S. Taverna (Eds.), *Patch-Clamp Methods and Protocols* (pp. 221–242). Springer New York.

Ting, J. T., Lee, B. R., Chong, P., Soler-Llavina, G., Cobbs, C., Koch, C., Zeng, H., & Lein, E. (2018). Preparation of Acute Brain Slices Using an Optimized N-Methyl-D-glucamine Protective Recovery Method. *Journal of Visualized Experiments: JoVE*, *132*. https://doi.org/10.3791/53825

Tischkau, S. A., Mitchell, J. W., Tyan, S.-H., Buchanan, G. F., & Gillette, M. U. (2003). Ca2+/cAMP response element-binding protein (CREB)-dependent

activation of Per1 is required for light-induced signaling in the suprachiasmatic nucleus circadian clock. *The Journal of Biological Chemistry*, *278*(2), 718–723.

Tong, Q., Ye, C.-P., Jones, J. E., Elmquist, J. K., & Lowell, B. B. (2008). Synaptic release of GABA by AgRP neurons is required for normal regulation of energy balance. *Nature Neuroscience*, *11*(9), 998–1000.

Trudeau, L.-E., Hnasko, T. S., Wallén-Mackenzie, A., Morales, M., Rayport, S., & Sulzer, D. (2014). The multilingual nature of dopamine neurons. *Progress in Brain Research*, *211*, 141–164.

Valdivia, S., Patrone, A., Reynaldo, M., & Perello, M. (2014). Acute high fat diet consumption activates the mesolimbic circuit and requires orexin signaling in a mouse model. *PloS One*, *9*(1), e87478.

van den Pol, A. N., Yao, Y., Fu, L.-Y., Foo, K., Huang, H., Coppari, R., Lowell, B. B., & Broberger, C. (2009). Neuromedin B and gastrin-releasing peptide excite arcuate nucleus neuropeptide Y neurons in a novel transgenic mouse expressing strong Renilla green fluorescent protein in NPY neurons. *The Journal of Neuroscience: The Official Journal of the Society for Neuroscience*, *29*(14), 4622–4639.

van den Top, M., Lee, K., Whyment, A. D., Blanks, A. M., & Spanswick, D. (2004). Orexigen-sensitive NPY/AgRP pacemaker neurons in the hypothalamic arcuate nucleus. *Nature Neuroscience*, *7*(5), 493–494.

van der Valk, E. S., van den Akker, E. L. T., Savas, M., Kleinendorst, L., Visser, J. A., Van Haelst, M. M., Sharma, A. M., & van Rossum, E. F. C. (2019). A

comprehensive diagnostic approach to detect underlying causes of obesity in adults. *Obesity Reviews: An Official Journal of the International Association for the Study of Obesity*, *20*(6), 795–804.

Varadarajan, S., Tajiri, M., Jain, R., Holt, R., Ahmed, Q., LeSauter, J., & Silver, R. (2018). Connectome of the Suprachiasmatic Nucleus: New Evidence of the Core-Shell Relationship. *eNeuro*, *5*(5). https://doi.org/10.1523/ENEURO.0205-18.2018

Verdejo-Román, J., Vilar-López, R., Navas, J. F., Soriano-Mas, C., & Verdejo-García, A. (2017). Brain reward system's alterations in response to food and monetary stimuli in overweight and obese individuals. *Human Brain Mapping*, *38*(2), 666–677.

Vong, L., Ye, C., Yang, Z., Choi, B., Chua, S., Jr, & Lowell, B. B. (2011). Leptin action on GABAergic neurons prevents obesity and reduces inhibitory tone to POMC neurons. *Neuron*, *71*(1), 142–154.

Wang, C.-Y. (2017). Circadian Rhythm, Exercise, and Heart. *Acta Cardiologica Sinica*, *33*(5), 539–541.

Wang, C.-Y., & Liao, J. K. (2012). A mouse model of diet-induced obesity and insulin resistance. *Methods in Molecular Biology* , *821*, 421–433.

Wang, J.-H., Wang, F., Yang, M.-J., Yu, D.-F., Wu, W.-N., Liu, J., Ma, L.-Q., Cai, F., & Chen, J.-G. (2008). Leptin regulated calcium channels of neuropeptide Y and proopiomelanocortin neurons by activation of different signal pathways. *Neuroscience*, *156*(1), 89–98.

Weaver, D. R. (1998). The suprachiasmatic nucleus: a 25-year retrospective. *Journal of Biological Rhythms*, *13*(2), 100–112.

Wei, W., Pham, K., Gammons, J. W., Sutherland, D., Liu, Y., Smith, A., Kaczorowski, C. C., & O'Connell, K. M. S. (2015). Diet composition, not calorie intake, rapidly alters intrinsic excitability of hypothalamic AgRP/NPY neurons in mice. *Scientific Reports*, *5*, 16810.

Welsh, D. K., Yoo, S.-H., Liu, A. C., Takahashi, J. S., & Kay, S. A. (2004). Bioluminescence imaging of individual fibroblasts reveals persistent, independently phased circadian rhythms of clock gene expression. *Current Biology: CB*, *14*(24), 2289–2295.

West, A. C., & Bechtold, D. A. (2015). The cost of circadian desynchrony: Evidence, insights and open questions. *BioEssays: News and Reviews in Molecular, Cellular and Developmental Biology*, *37*(7), 777–788.

Whitt, J. P., Montgomery, J. R., & Meredith, A. L. (2016). BK channel inactivation gates daytime excitability in the circadian clock. *Nature Communications*, *7*, 10837.

Wise, R. A. (2006). Role of brain dopamine in food reward and reinforcement. *Philosophical Transactions of the Royal Society of London. Series B, Biological Sciences*, *361*(1471), 1149–1158.

Wright, S. M., & Aronne, L. J. (2012). Causes of obesity. *Abdominal Imaging*, *37*(5), 730–732.

Xu, A. W., Kaelin, C. B., Takeda, K., Akira, S., Schwartz, M. W., & Barsh, G. S.

(2005). PI3K integrates the action of insulin and leptin on hypothalamic neurons. *The Journal of Clinical Investigation*, *115*(4), 951–958.

Yang, M.-J., Wang, F., Wang, J.-H., Wu, W.-N., Hu, Z.-L., Cheng, J., Yu, D.-F., Long, L.-H., Fu, H., Xie, N., & Chen, J.-G. (2010). PI3K integrates the effects of insulin and leptin on large-conductance Ca2+-activated K+ channels in neuropeptide Y neurons of the hypothalamic arcuate nucleus. *American Journal of Physiology. Endocrinology and Metabolism*, *298*(2), E193–E201.

Yan, L., & Silver, R. (2016). Neuroendocrine underpinnings of sex differences in circadian timing systems. *The Journal of Steroid Biochemistry and Molecular Biology*, *160*, 118–126.

Yi, M., Li, H., Wu, Z., Yan, J., Liu, Q., Ou, C., & Chen, M. (2018). A Promising Therapeutic Target for Metabolic Diseases: Neuropeptide Y Receptors in Humans. *Cellular Physiology and Biochemistry: International Journal of Experimental Cellular Physiology, Biochemistry, and Pharmacology*, *45*(1), 88–107.

Zabeau, L., Verhee, A., Catteeuw, D., Faes, L., Seeuws, S., Decruy, T., Elewaut, D., Peelman, F., & Tavernier, J. (2012). Selection of non-competitive leptin antagonists using a random nanobody-based approach. *Biochemical Journal*, *441*(1), 425–434.

Zarrinpar, A., Chaix, A., & Panda, S. (2016). Daily Eating Patterns and Their Impact on Health and Disease. *Trends in Endocrinology and Metabolism: TEM*, *27*(2), 69–83.

Zhang, S. X., Lutas, A., Yang, S., Diaz, A., Fluhr, H., Nagel, G., Gao, S., & Andermann, M. L. (2021). Hypothalamic dopamine neurons motivate mating through persistent cAMP signalling. *Nature*, 1–5.

Zhang, X., & van den Pol, A. N. (2016). Hypothalamic arcuate nucleus tyrosine hydroxylase neurons play orexigenic role in energy homeostasis. *Nature Neuroscience*, *19*(10), 1341–1347.

Zhang, Y., Proenca, R., Maffei, M., Barone, M., Leopold, L., & Friedman, J. M. (1994). Positional cloning of the mouse obese gene and its human homologue. *Nature*, *372*(6505), 425–432.

Zhao, M., Jung, Y., Jiang, Z., & Svensson, K. J. (2020). Regulation of Energy Metabolism by Receptor Tyrosine Kinase Ligands. *Frontiers in Physiology*, *11*, 354.

Zhao, Z.-D., Yang, W. Z., Gao, C., Fu, X., Zhang, W., Zhou, Q., Chen, W., Ni, X., Lin, J.-K., Yang, J., Xu, X.-H., & Shen, W. L. (2017). A hypothalamic circuit that controls body temperature. *Proceedings of the National Academy of Sciences of the United States of America*, *114*(8), 2042–2047.